NASA-CR-178974

P-118

AEROJET STRATEGIC PROPULSION COMPANY
P.O. BOX 15699C
SACRAMENTO, CALIFORNIA 95813

SRB/SLEEC (SOLID ROCKET BOOSTER/ SHINGLE LAP EXTENDIBLE EXIT CONE) FEASIBILITY STUDY

Period of Performance
23 September 1985 to 19 September 1986

Published 19 September 1986

FINAL REPORT
Contract NAS8-36571
Report No. SRB-CLE-F

Volume 2 of 2 Volumes

APPENDIX A

DESIGN STUDY FOR A SLEEC ACTUATION SYSTEM

Prepared by

Garrett Pneumatic Systems Division
Tempe, Arizona 85282

(NASA-CR-178974) SRB/SLEEC (SOLID ROCKET BOOSTER/SHINGLE LAP EXTENDIBLE EXIT CONE) FEASIBILITY STUDY, VOLUME 2. APPENDIX A: DESIGN STUDY FOR A SLEEC ACTUATION SYSTEM Final Report, 23 Sep. 1985 - 19 Sep. (Aerojet G3/20 N88-28965 Unclas 0164895

[redacted] Date for general release Sept. 1988.

Prepared for

GEORGE C. MARSHALL SPACE FLIGHT CENTER
MARSHALL SPACE FLIGHT CENTER, ALABAMA 35812

(NASA-CR-17[illegible] Vol-2) SRB/SLEEC (SOLID ROCKET BOOSTER/SHINGLE LAP EXTENDIBLE EXIT CONE) FEASIBILITY STUDY, VOLUME 2 Final Report, [illegible] Sep. 1985 - 19 Sep. 1986 (Garrett Corp.) [illegible] LIMIT DISTRIB [illegible] Unclas [illegible]

DESIGN STUDY

FOR AEROJET STRATEGIC PROPULSION COMPANY

FOR A SLEEC ACTUATION SYSTEM TO BE USED ON THE SPACE TRANSPORTATION SYSTEM

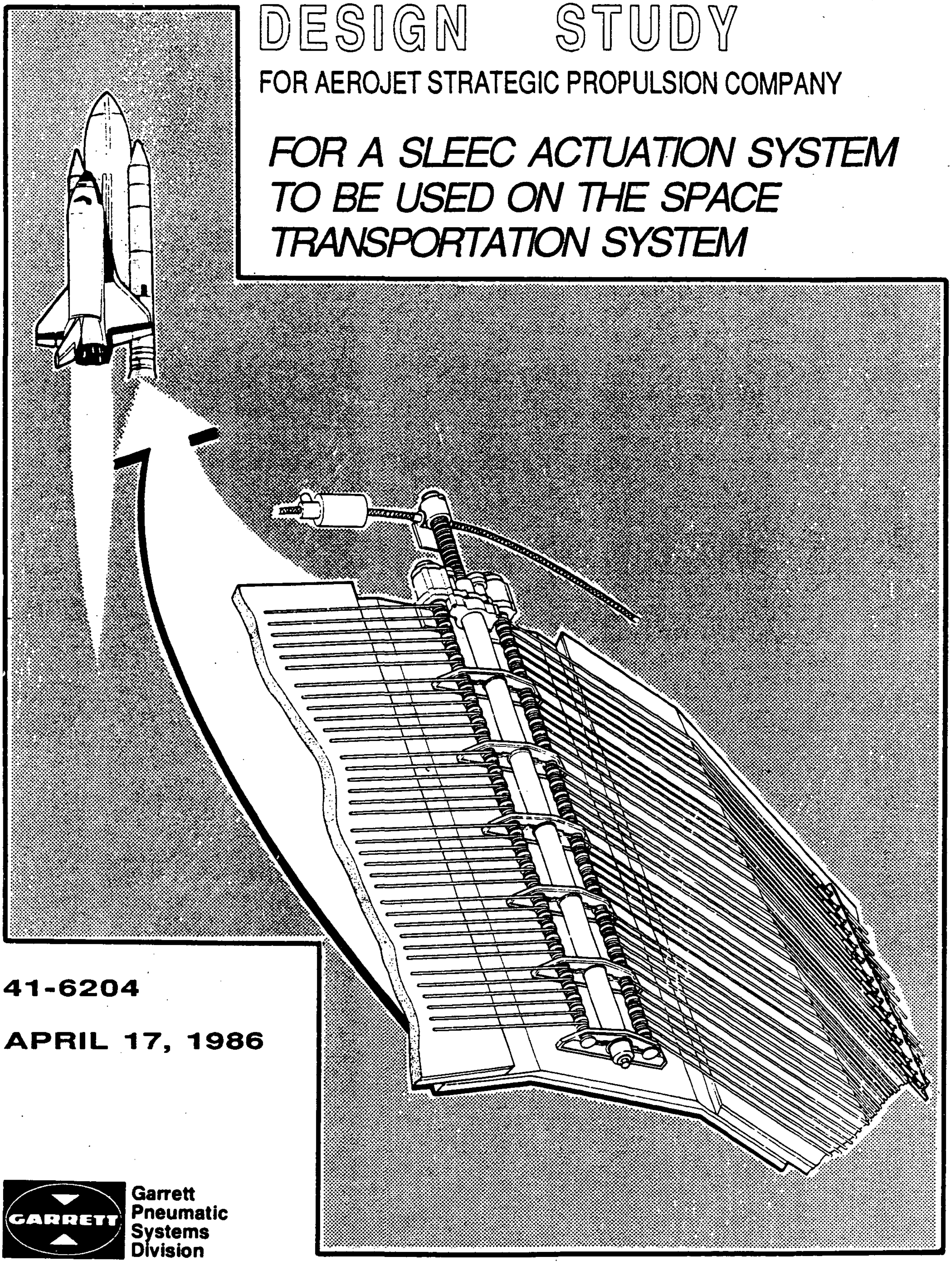

41-6204

APRIL 17, 1986

GARRETT
Garrett
Pneumatic
Systems
Division

DESIGN STUDY
FOR AEROJET STRATEGIC PROPULSION COMPANY
FOR A SLEEC ACTUATION SYSTEM
TO BE USED ON THE
SPACE TRANSPORTATION SYSTEM

41-6204 April 17, 1986

Prepared by D. S. Thompson

Initial Issue
Approved by

for J. W. Shaw/Supervisor,
Engineering Publications

J. Tervo/Design Engineer

E. Schall/Engineering Sciences

J. Merritt/Program Engineer

C. G. Trowbridge/Sr. Proj. Engr.

GARRETT PNEUMATIC SYSTEMS DIVISION
A DIVISION OF THE GARRETT CORPORATION
1300 W. WARNER RD. P.O. BOX 22200
TEMPE, ARIZONA 85282 TEL (602) 893-9423

TABLE OF CONTENTS

TABLE OF CONTENTS (CONTD.)

LIST OF ATTACHMENTS

LIST OF TABLES

LIST OF FIGURES

LIST OF FIGURES (CONTD)

Introduction and Summary

DESIGN STUDY FOR AEROJET STRATEGIC PROPULSION COMPANY FOR A SLEEC ACTUATION SYSTEM TO BE USED ON THE SPACE TRANSPORTATION SYSTEM

SECTION 1

INTRODUCTION AND SUMMARY

1.1 INTRODUCTION

This document, prepared by Garrett Pneumatic Systems Division (GPSD) of The Garrett Corporation, Tempe, Arizona, presents the results of a design feasibility study of a self-contained (powered) actuation system for a Shingle Lap Extendible Exit Cone (SLEEC) for use on the Solid Rocket Boosters (SRB) used in the NASA-MSFC Space Transportation System (STS). The design study was conducted for Aerojet Strategic Propulsion Company (ASPC), Sacramento, California, in accordance with the ASPC Statement of Work (SOW) SRB-CLE-01, dated 15 October 1985 and is submitted to ASPC.

1.2 SUMMARY

This report reviews the evolution of the SLEEC actuation system design, summarizes the final design concept, and presents the results of the detailed study of the final concept of the actuation system.

During the study, technical interface (TI) meetings between ASPC and GPSD were held. The meetings were an important part in resolving the final design concept, and they also clarified certain requirements of the SOW: Scaling up of the earlier SLEEC design was found to be impractical; redundancy for the actuator system except for drive motor/brake and flexible drive shafts was omitted due to design restrictions and weight considerations; and, system recovery and refurbishment capability was deleted as being impractical.

A conservative design using proven mechanical components was established as a major program priority. The final mechanical design has a very low development risk since the components, which consist of ballscrews, gearing, flexible shaft drives, and aircraft cables, have extensive aerospace applications and a history of proven reliability.

The mathematical model studies have shown that little or no power is required to deploy the SLEEC actuation system because acceleration forces and internal pressure from the rocket plume provide the required energies. A speed control brake is incorporated in the design in order to control the rate of deployment.

As defined during the ASPC/GPSD TI meetings and the SOW, an estimate of component weight, a system and component reliability study, and assembly drawings are contained within this report. Cost estimates for 25, 50, and 100 units are being transmitted under separate cover. Interfacing the actuation system to the SRB and shingles was accomplished during the TI meetings.

Design

SECTION 2

DESIGN

2.1 DESIGN SUMMARY

ASPC Statement of Work SRB-CLE-01 called for a "scale-up" in size of the successful subscale SLEEC which was deployed and test fired for 20 seconds on the Super BATES motor. The conceptual portion of the design study, however, revealed that a simple scaling up was not feasible. The weight, complexity, potential binding, and lack of shingle support were unmanageable problems inherent in a system utilizing two or three circumferential ballscrew actuator drives to restrain and program the movement of the inner and outer shingles during deployment. The nature of the main axial ballscrew drive suggested that a roll out of aircraft cable could control the radial expansion of the shingles during deployment and also uniformily support the shingles over their lengths with the least possible system weight. Table 2-1 at the end of this section presents the SLEEC system design weights. Since cables only perform in tension it was necessary to determine if tension could be maintained at all times. Analysis revealed that, within the confines of the mission profile the cables would always be in tension as a result of the internal pressure from the rocket exhaust plume. This positive pressure together with the g-load from acceleration are more than sufficient to drive the system to full deployment once the stow lock brake is released.

Drive motors are included in order to assure that the system has adequate potential to overcome breakaway friction at the start of the deployment. Also included are speed control drag brakes to regulate the rate of deployment. Figure 2-1 is a cutaway view showing one-sixth of the SLEEC actuation system.

2.2 COMPONENT DETAILS AND OPERATION

The SLEEC actuation system consists of six actuation assemblies, four short flexible shaft assemblies, four long flexible shaft assemblies, and two drive motor/brake assemblies as shown on the four sheets of Garrett drawing L860527 attached at the end of this section.

Each actuation assembly is mounted to the exterior of an inner shingle as shown in Figure 2-1, and contains a 1.750-inch-diameter ballscrew and nut assembly which provides the axial drive force to the system. This ballscrew and nut assembly is driven by a 10:1 worm-gear set. As the ballscrew rotates, it imparts rotation to two 37.5:1 differential gearboxes through a 1.000-inch-diameter spline

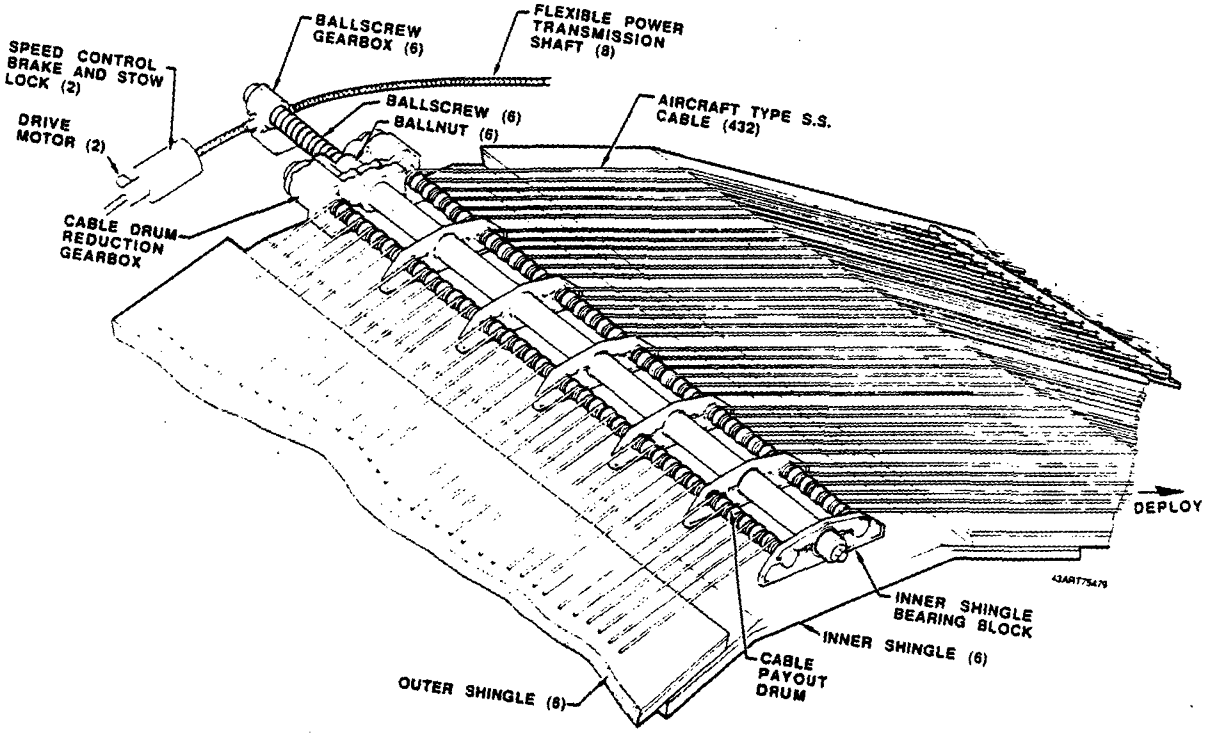

FIGURE 2-1

ONE-SIXTH SLEEC CUTAWAY VIEW

shaft, a ball nut guide, and two sets of spur gears. It should be noted that the two differential gearboxes rotate in opposite directions, thus necessitating an idler gear prior to the differential gearbox input shaft on one side.

The actuation assemblies also contain two cable drums coupled directly to the output of the differential gearboxes. These drums provide radial constraint to the outer shingles by means of 0.1875-inch-diameter cables attached to the drums and to the outer shingles. One of the cable drums has a left-hand helix cable groove, or left-hand lay. The other cable drum has a right-hand helix cable groove, or right-hand lay, to ensure symmetrical loading of the entire system as the cable is payed off the drums.

The cables, which provide radial constraint to the outer shingles, are attached to the cable drums by means of balls swaged to the cable ends. These ball ends are placed into recesses machined into the cable drums and held there by retaining rings which are snapped over the drum and ball assemblies. Note that the ball/cable joint is not subjected to high loading because two wraps of the cable remain on the drum at full deployment.

Threaded sleeves are swaged to the cable ends not attached to the cable drums. These sleeves are threaded over tie rods which attach opposing cables on the same axis (see Section F-F on Sheet 3 of Drawing L860527). After the cables are pre-tensioned, the tie rods are rigidly attached to T-bars fastened to each outer shingle. Adjustability and ease of assembly are provided by this configuration.

The drive motor/brake assembly is the power source which supplies and controls the rotation necessary for deployment. These drive motor/brake assemblies also have a braking mechanism which controls the rate of deployment. Either of the two drive/motor brake assemblies has the capability of deploying the system and thus provides a redundant power transfer to the actuation assemblies through a complete loop of flexible drive shafts.

External hydraulic or electrical power (depending on availability) is supplied to the drive motor/brake assembly which rotates the input shaft of the worm gear set through the flexible drive shafts. The worm gear set then rotates the ballscrew and connected spline shaft causing axial translation. Simultaneously, the splined shaft rotates the ballscrew guide and its attached gear. The attached gear then drives the differential gearbox input shafts by means of the spur gear sets. For the gear arrangement and direction of rotation see Sheet 4 of Drawing L860527. The differential gearboxes are coupled directly to the cable drums which cause the drums to rotate and pay the cables off the drums, allowing radial deployment of the shingles. Axial deployment force is imparted to the outer shingles by means of drive plates attached to the forward ends of the inner shingles.

Section A-A of Sheet 1 of Drawing L860527 shows the stowed and extended views of the actuation system and illustrates that all actuation components, except the ballscrew and its drive gear head, are mounted on the inner shingle and extend with it.

The change in cable angle shown on Sheet 1 of Drawing L860527 causes an increase in cable tension, compensating for stretch in the cables due to higher loading during deployment.

Cable lead compensating screws can be incorporated into the cable drums if the change in angle to the centerline of the cable drum will adversely affect the performance of the system.

TABLE 2-1

SLEEC WEIGHT ANALYSIS

Item Number*	Description	Unit Weight lbs	Quantity	Total Weight lbs
1	Thrust Plate	0.086	6	0.520
2	Hex Nut	0.065	6	0.393
3	Cover	0.037	6	0.226
4	End Cap	1.067	6	6.404
5	Thrust Bearing	0.399	6	2.394
6	Needle Bearing	0.962	6	5.772
7	Woodruff Key	0.004	6	0.024
8	Worm Wheel	0.773	6	4.642
9	Worm	0.596	6	3.578
10	Thrust Collar	0.543	6	3.263
11	Drive Shaft	1.455	6	8.731
12	Retaining Pin	0.019	6	0.115
13	Bushing	0.423	6	2.542
14	Spur Gear	0.906	6	5.438
15	Spur Gear	0.495	12	5.947
16	Spur Gear	0.375	6	2.250
17	Spur Gear	0.279	6	1.674
18	Spur Gear	0.238	6	1.431
19	Spur Gear	0.375	6	2.250
20	Spur Gear	0.238	6	1.431
21	Ball Screw Guide	12.158	6	72.949
22	Bearing Block	1.543	36	55.573
23	Front Housing	1.053	6	6.323
24	End Cap	0.235	12	2.827
25	Cable Retainer	0.037	432	15.940
26	Ball Screw	17.318	6	103.910
27	Ball Nut	4.400	6	26.401
28	Worm Gear Housing	4.809	6	28.854
29	Ball Bearing	0.160	84	13.440
30	Pad Bearing	0.003	72	0.204
31	Planet Gear	0.620	72	44.647
32	Sun Gear	0.860	12	10.321
33	Ring Gear	1.500	12	18.004
34	Fixed Ring Gear	5.144	12	61.726
35	Mounting Bracket	16.225	6	97.355
36	Right Rear Housing	0.519	6	3.112
37	Spline Shaft	9.138	6	54.828
38	Bolt	0.088	6	0.529
39	Washer	0.059	6	0.354

TABLE 2-1 (CONT.)

SLEEC WEIGHT ANALYSIS

Item Number*	Description	Unit Weight lbs	Quantity	Total Weight lbs
40	Cable	0.183	432	79.000
41	Flex Shaft	1.257	8	10.053
42	Cable Drum	24.60	12	295.21
43	Left Rear Housing	0.693	6	4.156
44	Motor/Brake Drive	3.000	2	6.000
45	T-Bar	3.230	6	19.380
46	Tie-Rod	0.052	216	11.232
47	Hex-Nut	0.011	432	4.752
	Miscellaneous			12.00
	Calculated Actuation System Weight			1118.105

* These numbers correspond to the find numbers on Sheet 1 of Garrett Drawing L860527.

ORIGINAL PAGE IS
OF POOR QUALITY

2 FOLDOUT FRAME

DATUM	LAST SEQ LTR USED
LOCATION	ALSO USED

REVISION STATUS OF SHEETS

REVISIONS: ZONE | LTR | DESCRIPTION | DATE | APPROVED

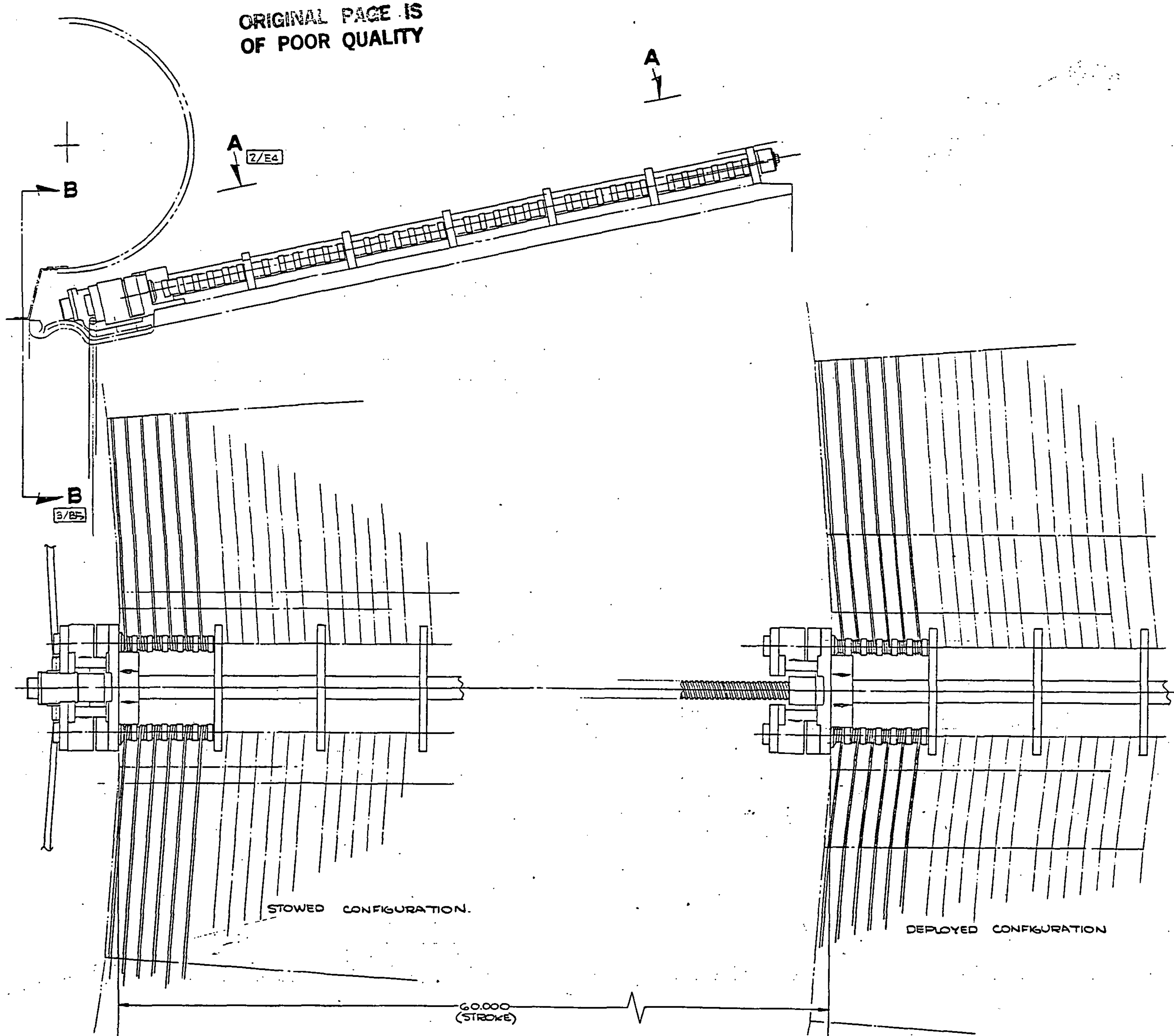

VIEW **A-A**

QUANTITY REQD	FIND NO	PART NO OR IDENTIFYING NO	SYM	NOMENCLATURE OR DESCRIPTION	FSCM NO	MATERIAL AND SPECIFICATION	ZONE
432	47			HEX NUT		CRES	
216	46			TIE ROD		CRES	
6	45			TEE BAR		ALUM	
2	44			MOTOR/BRAKE DRIVE			
6	43			HOUSING, REAR, LEFT		ALUM CSTG	
12	42			DRUM, CABLE		STL, 4340	
8	41			FLEX SHAFT ASSY		CORE CRES	
432	40			CABLE, 3/16 DIA		CRES MIL-W-83420D (TYPE I COMP B)	
6	39			WASHER		CRES	
6	38			BOLT, HEX HEAD		CRES	
6	37			SPLINE SHAFT		STL, 4340	
6	36			HOUSING, REAR, RT		ALUM CSTG	
6	35			BRACKET, MAIN MTG		CRES, 17-4 CSTG	
6	34			RING GEAR, FIXED		STL, 9310	
6	33			RING GEAR		STL, 9310	
6	32			SUN GEAR		STL, 9310	
36	31			PLANET		STL, 9310	
72	30			BEARING PAD		PTFE	
84	29	7104		BEARING, BALL		CRES	
6	28			HOUSING, WORM GEAR		CRES, 17-4, CSTG	
6	27			BALL NUT		STL	
6	26			BALL SCREW		STL	
432	25			RETAINER, CABLE		ALUM	
24	24			CAP, END		STL, 4340	
6	23			HOUSING, FRONT		ALUM CASTING	
36	22			BEARING BLOCK		ALUM CASTING	
6	21			GUIDE, BALL SCR		CRES, 15-5	
6	20			SPUR GEAR		STL, 9310	
6	19			SPUR GEAR		STL, 9310	
6	18			SPUR GEAR		STL, 9310	
6	17			SPUR GEAR		STL, 9310	
6	16			SPUR GEAR		STL, 9310	
6	15			SPUR GEAR		STL, 9310	
6	14			SPUR GEAR		STL, 9310	
12	13			BUSHING		STL BACKED PTFE/BRNZ	
12	12			PIN, RETAINING		CRES, 300 SERIES	
6	11			SHAFT, DRIVE		STL, 4340	
6	10			THRUST COLLAR		CRES, 440-C	
6	9			WORM		STL, 4340	
6	8			WORM WHEEL		STL, 4340	
12	7			WOODRUFF KEY		STL	
66	6			NEEDLE BRG		STL	
45	5			NEEDLE THRUST BRG		STL	
6	4			END CAP		STL, 4340	
6	3			COVER		CRES, 17-4 PH	
6	2			NUT, HEX .625-18		CRES, 300 SERIES	
6	1			PLATE, THRUST		CRES, 440-C	

← DASH NUMBER   PARTS LIST

REQD	NEXT ASSY	USED ON	CONTRACT NO		
HEAT TREATMENT		PROCESS	SIGNATURE	DATE	
HARDNESS AND SPEC		NAME AND SPEC	DFT TERVO	86-03-13	
			CHK		
			MFG		
			MATL		
DESIGN ACTIVITY APPD		DATE 86-04-07	STRESS L.M. Schall	86-4-08	
OTHER ACTIVITY APPD		DATE	AERO		
			QA		
			APPD	86-04-08	

GARRETT PNEUMATIC SYSTEMS DIVISION
A DIVISION OF THE GARRETT CORPORATION
PHOENIX, ARIZONA

DWG TITLE: SLEEC
SHINGLE LAP
EXTENDIBLE EXIT CONE

SIZE	FSCM NO	DWG NO
E	59364	L860527
SCALE 1/4	WT	SHEET 1 OF 3

FOLDOUT FRAME

NO DWG L860527 SHEET 1 OF 3

6P100-50

ORIGINAL PAGE IS
OF POOR QUALITY

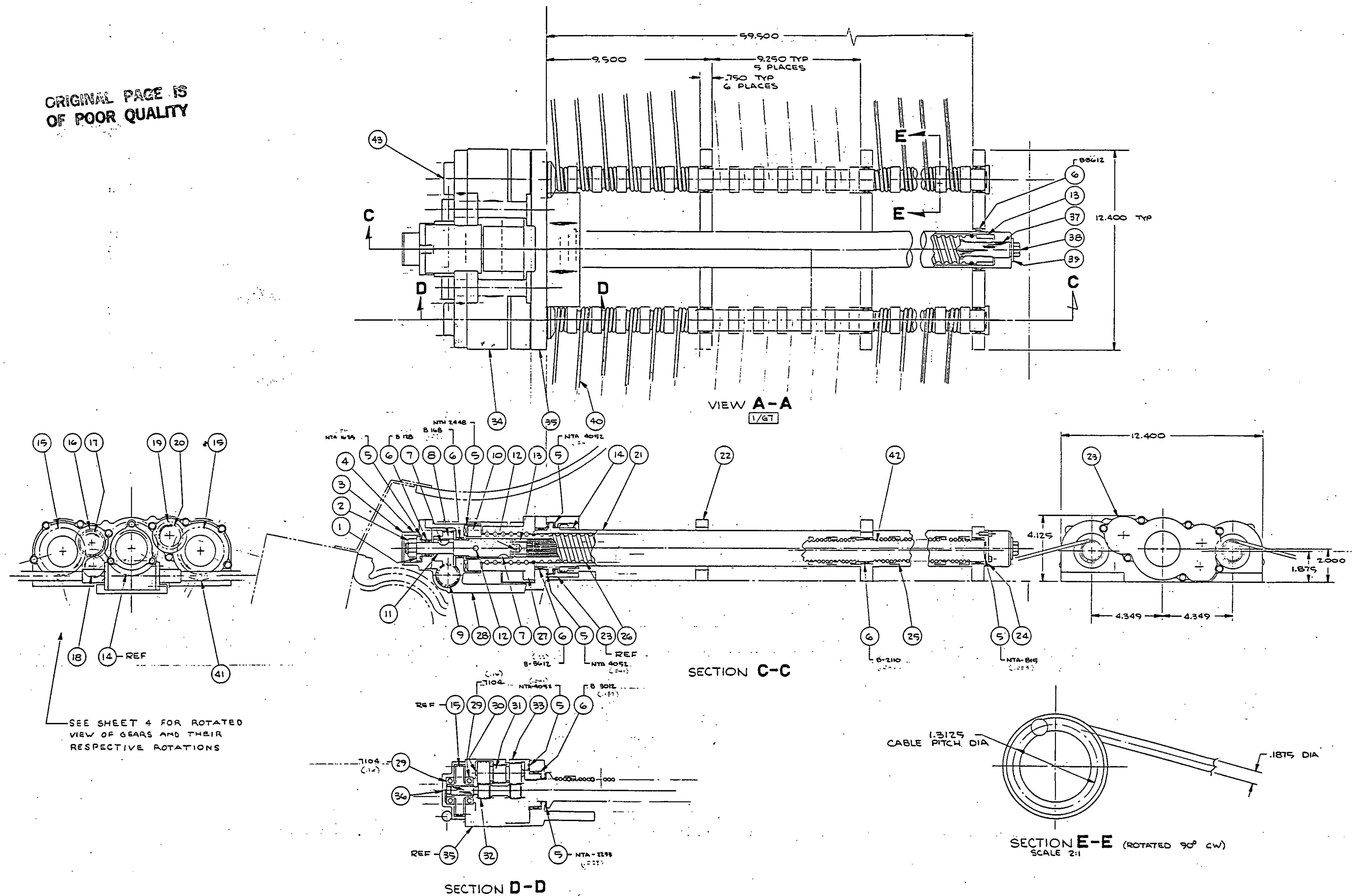

FOLDOUT FRAME

2 FOLDOUT FRAME

SIZE E	FSCM NO 59364	DWG NO L860527
SCALE 1/2 & NOTED	REV	SHEET 2 OF 3

SEE SHEET 1 FOR CONTROLLING REV LTR

DWG NO L860527 SHEET 2 OF 3

ORIGINAL PAGE IS
OF POOR QUALITY

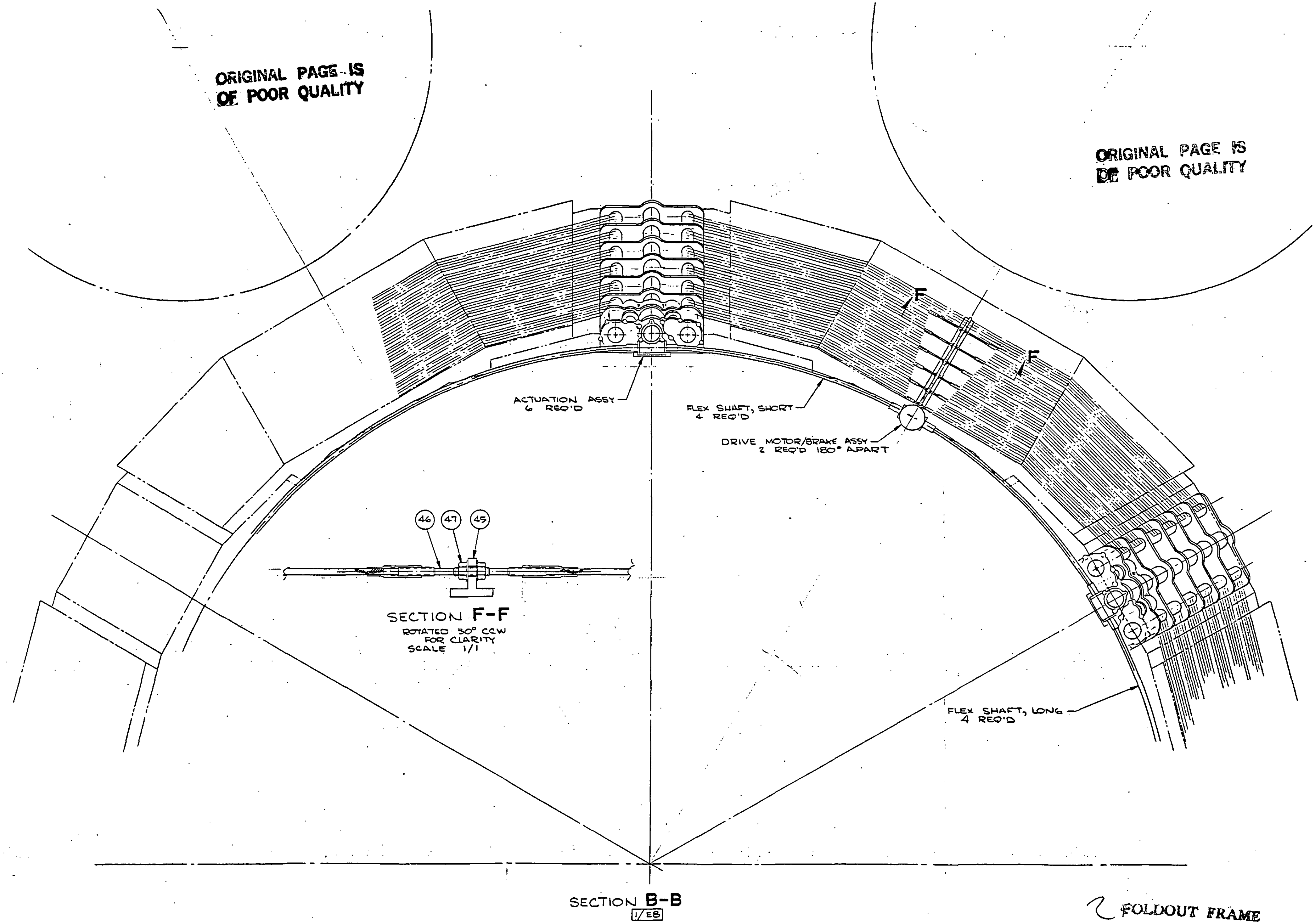

FOLDOUT FRAME

FOLDOUT FRAME

SEE SHEET 1 FOR CONTROLLING REV LTR

SIZE	FSCM NO	DWG NO
E	59364	L860527
SCALE 1/4	REV	SHEET 3 OF 3

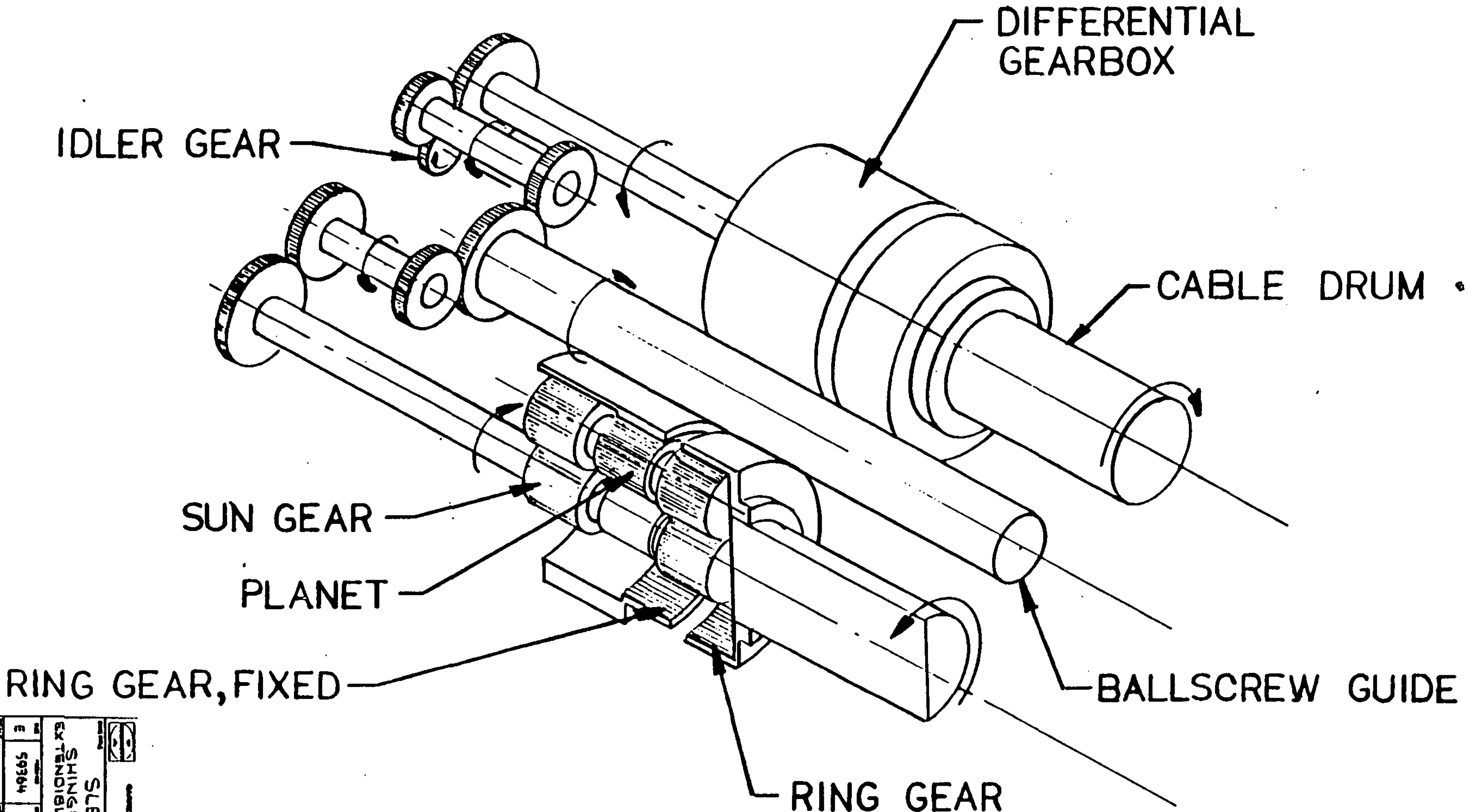

SLEEC
SHINGLE LAP
EXTENDIBLE EXIT CONE
E 59364 L860527
1/4

Performance

SECTION 3

PERFORMANCE

3.1 PERFORMANCE SUMMARY

A computer model of the SLEEC actuation system has been developed and used to simulate system performance. The computer model includes the effects of system inertia, friction, and external loading on the system during deployment. Based on the predicted acceleration loads and assumed system frictions during in-flight operation, the analysis indicates that driving motors are probably not required for deployment. However, they have been retained in the design to provide any necessary system input required due to unexpected variations in friction and for peak transient loads. The motor is also used during ground check-out. A braking mechanism has been incorporated into the design which will control the rate of deployment during the flight profile.

3.2 SYSTEM PERFORMANCE

The performance of the SLEEC actuation system was predicted by a computer simulation of the system dynamics. The heart of the simulation is a predictor-corrector integration routine with a variable step size to provide accuracy and execution speed. A block diagram of this computer simulation is provided in Figure 3-1. As shown, the motor acceleration is determined by the sum of load, drag, brake, and motor torques. The motor shaft velocity is determined by integrating acceleration; similarly, position is the integral of velocity. The axial and radial (i.e., circumferential) positions of the inner and outer shingles are found by reflecting the motor position through the appropriate gear trains.

The key components of the model include 1) a small electric motor represented by a torque-speed curve, 2) load maps based on predicted axial and radial loads as a function of displacement, 3) a load map representing the brake torque as a function of motor speed, and 4) the gear ratios necessary to deploy the shingles 60 inches axially and 6.6 inches circumferentially per cable roller (resulting in a total circumferential cone expansion of 79.2 inches) in thirteen seconds with an average motor speed of 2770 rpm.

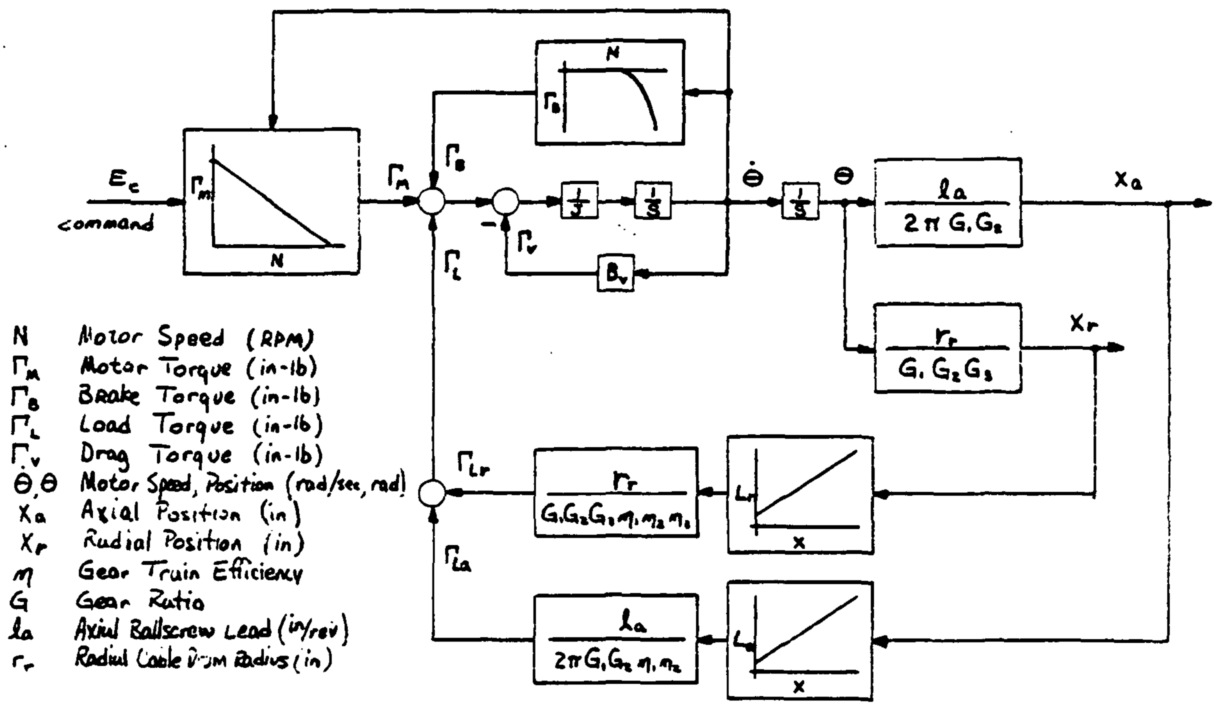

FIGURE 3-1

COMPUTER MODEL BLOCK DIAGRAM
OF THE SLEEC ACTUATION SYSTEM

Each of the two motors was selected based on its capability to deploy the system in 20 seconds during a ground checkout. A 0.2 hp dc electric motor provides the necessary power to accomplish this. The required motor stall torque (25 in-lb) was determined from the load torques plus the torque required to accelerate the motor in the specified time during ground checkout. Motor freerun speed was selected as 2000 rpm. These values defined an approximate motor torque-versus-speed curve which was then used for the computer simulation.

The mechanical brake was sized to control the speed of the motor under aiding loads. The brake has no effect for speeds less than the motor freerun speed but provides a resistive torque equal to the square of the motor speed for speeds greater than the freerun speed. The brake supplies approximately 200 in-lb of resistive torque at the flight deployment speed of 2770 rpm.

The gear ratio (including the ballscrew lead and necessary gear reductions) was determined to be 10 revolutions of the motor per inch of axial shingle stroke. In the circumferential direction the gear ratio was determined to be 90.91 revolutions of the motor per inch of cable payed out.

Two loading cases were investigated for deployment of the system: 1) a ground checkout loading case, and 2) a predicted flight load case. The results of the computer simulation are summarized in Tables 3-1 and 3-2 for these cases. Performance plots of position, velocity, motor speed and mechanical energy are shown in Figures 3-2 through 3-5 for the ground checkout load case and in Figures 3-6 through 3-9 for the flight load case.

TABLE 3-1

SLEEC PERFORMANCE SUMMARY AT GROUND CHECKOUT LOADS

Parameter	Magnitude
Maximum motor speed (rpm)	1911
Maximum axial velocity (in/sec)	3.185
Maximum radial velocity (in/sec)	0.343
Impact translational energy (in-lb)	44.02
Impact rotational energy (in-lb)	721.21
Total kinetic energy (in-lb)	765.23
Deploy time (sec)	19.125

TABLE 3-2

SLEEC PERFORMANCE SUMMARY AT MAXIMUM FLIGHT LOADS

Parameter	Magnitude
Maximum motor speed (rpm)	2747
Maximum axial velocity (in/sec)	4.578
Maximum radial velocity (in/sec)	0.493
Impact translational energy (in-lb)	90.94
Impact rotational energy (in-lb)	1489.95
Total kinetic energy (in-lb)	1580.89
Deploy time (sec)	13.125

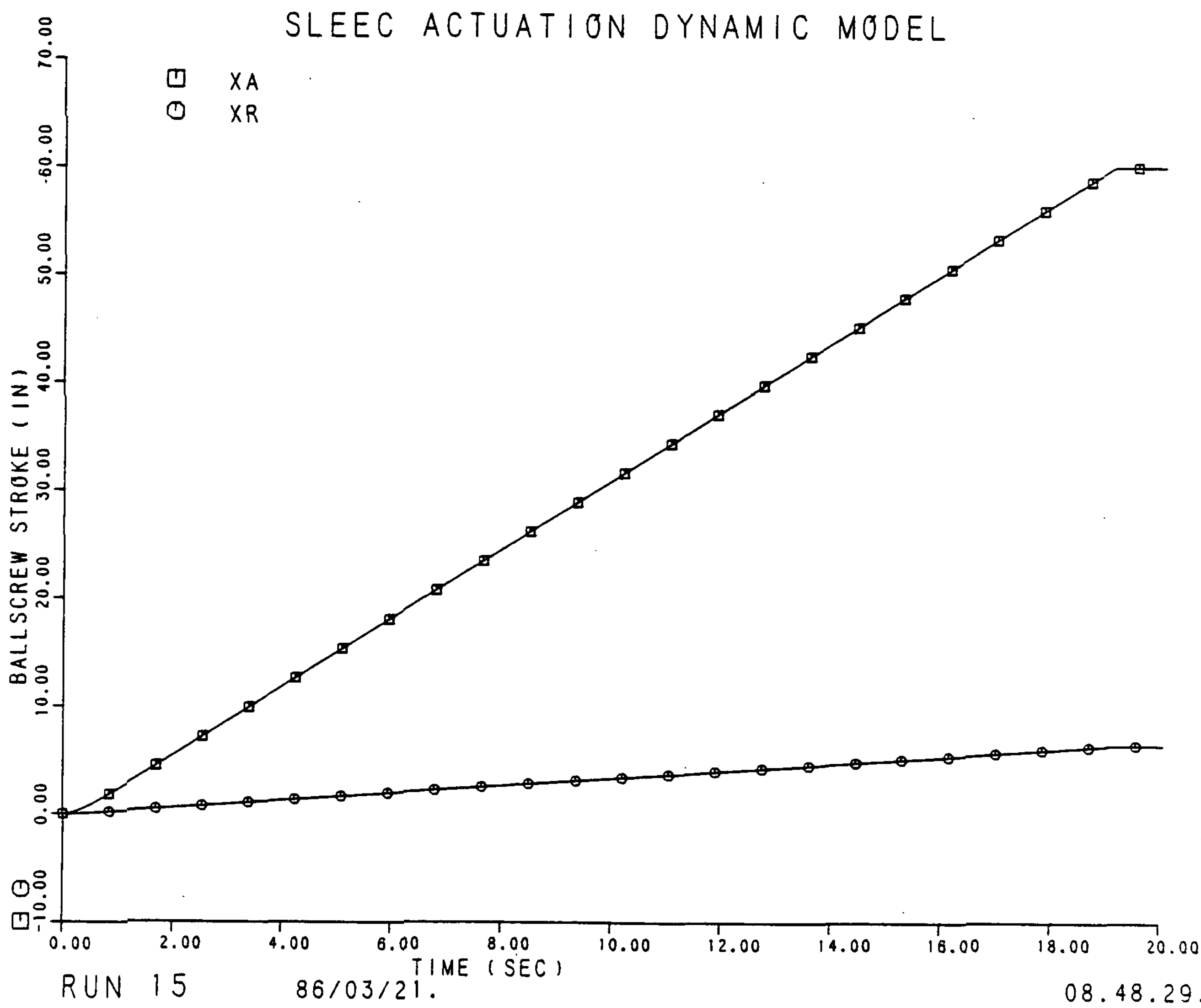

FIGURE 3-2

SLEEC PERFORMANCE SIMULATION OF AXIAL
AND RADIAL POSITION FOR GROUND CHECKOUT LOADS

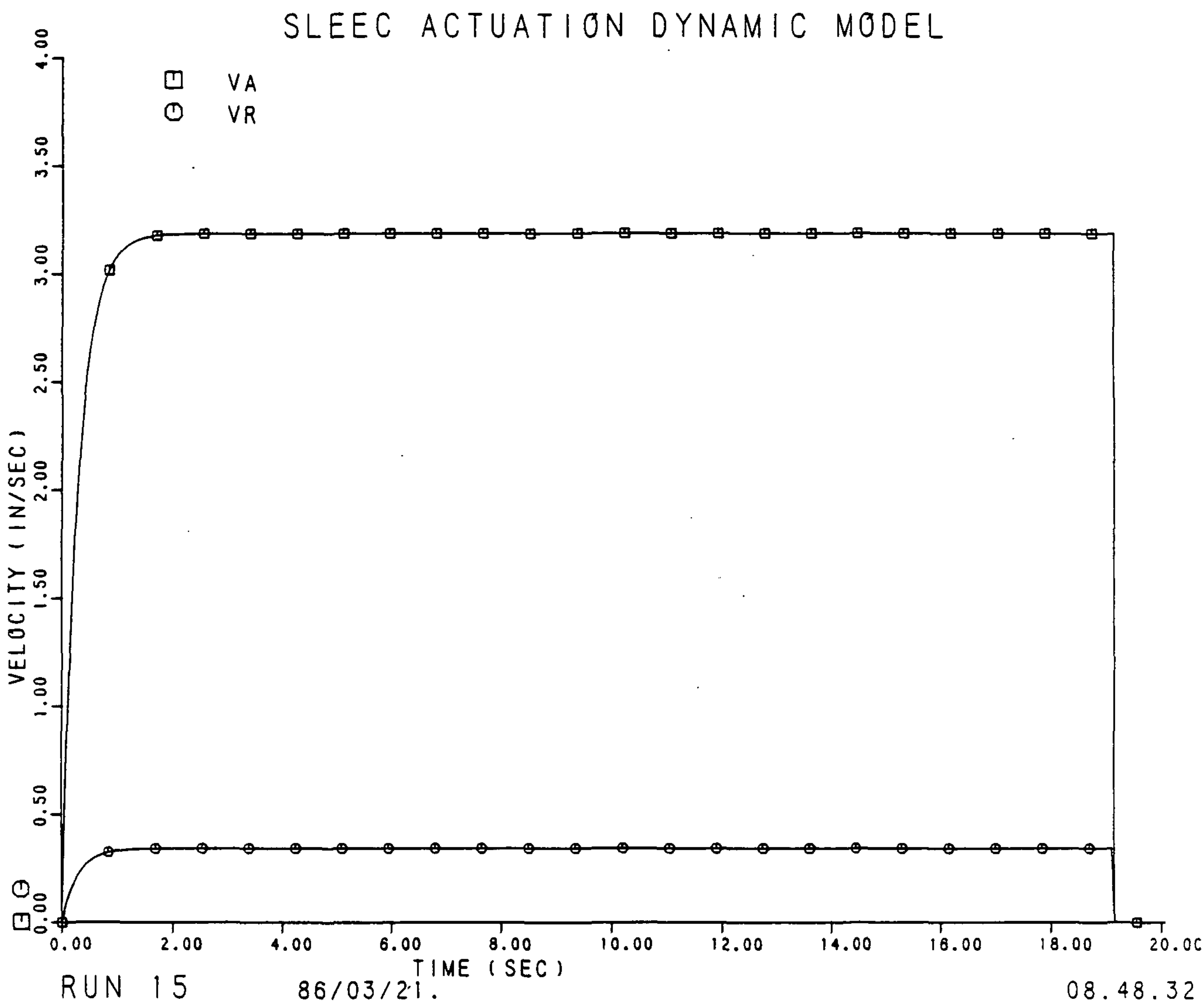

FIGURE 3-3

SLEEC PERFORMANCE SIMULATION OF AXIAL
AND RADIAL VELOCITY FOR GROUND CHECKOUT LOADS

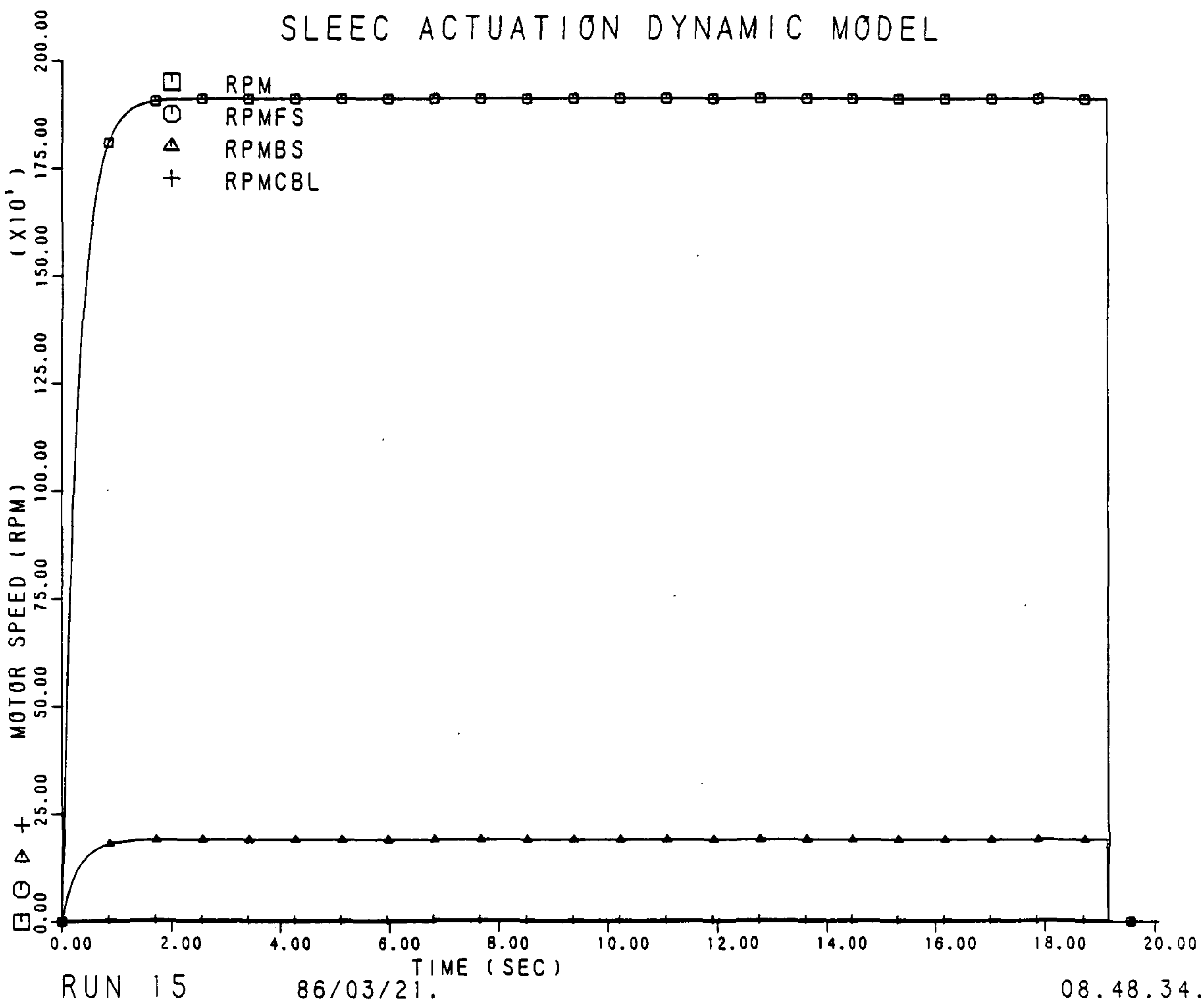

FIGURE 3-4

SLEEC PERFORMANCE SIMULATION OF MOTOR, FLEX SHAFT, BALLSCREW, AND CABLE DRUM SPEEDS FOR GROUND CHECKOUT LOADS

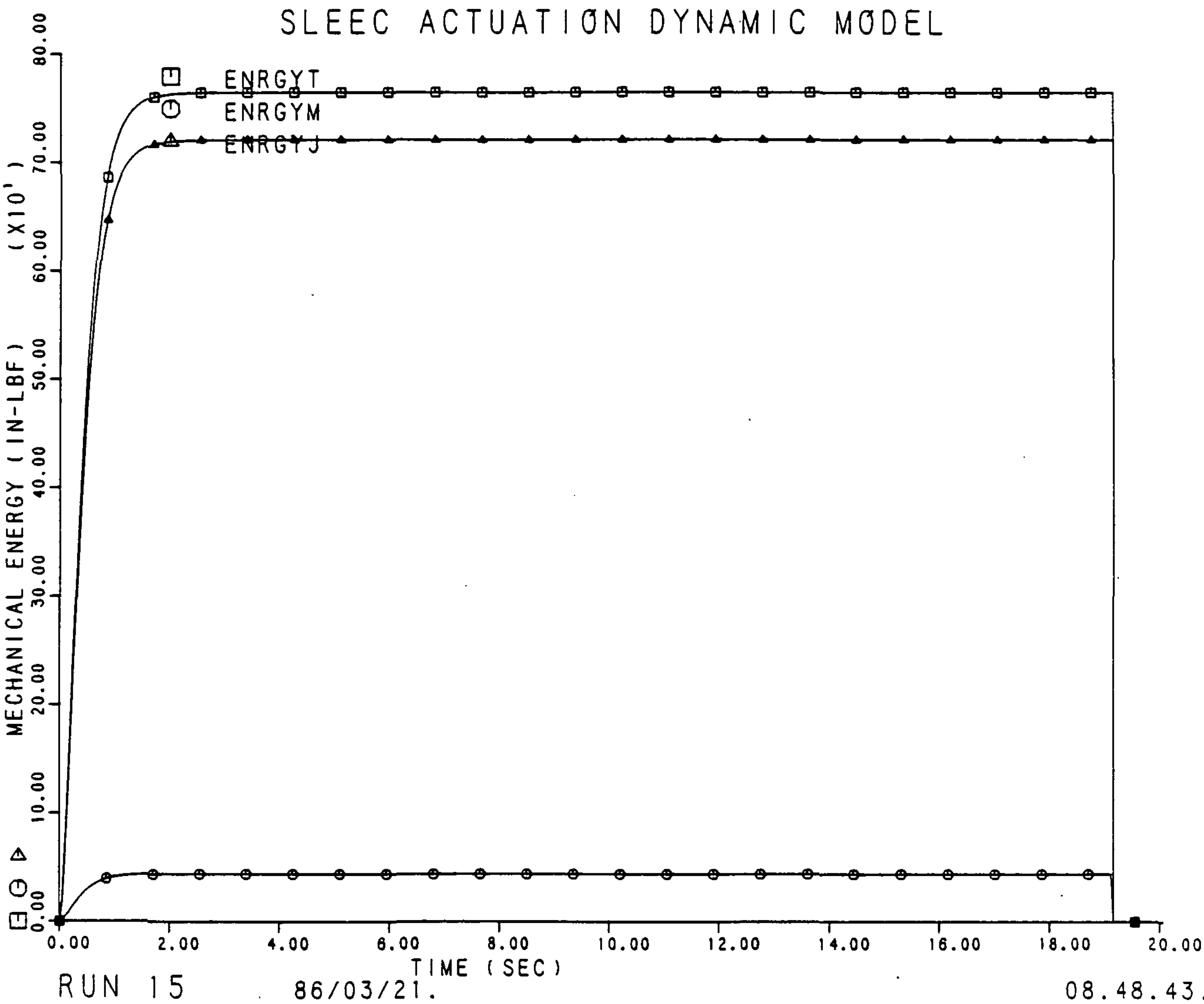

FIGURE 3-5

SLEEC PERFORMANCE SIMULATION OF IMPACT ENERGY FOR GROUND CHECKOUT LOADS

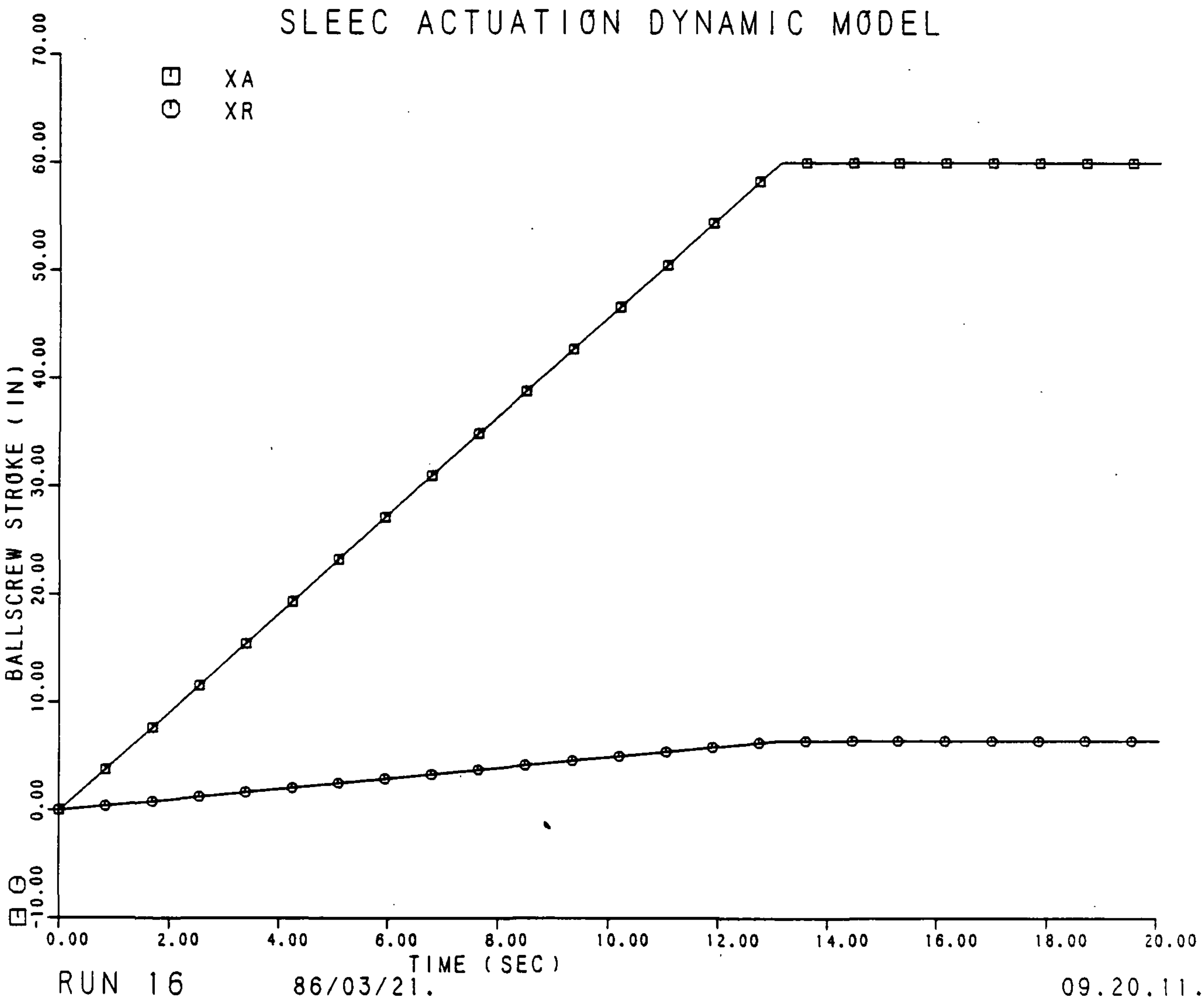

FIGURE 3-6

SLEEC PERFORMANCE SIMULATION OF AXIAL AND RADIAL POSITION FOR MAXIMUM FLIGHT LOADS

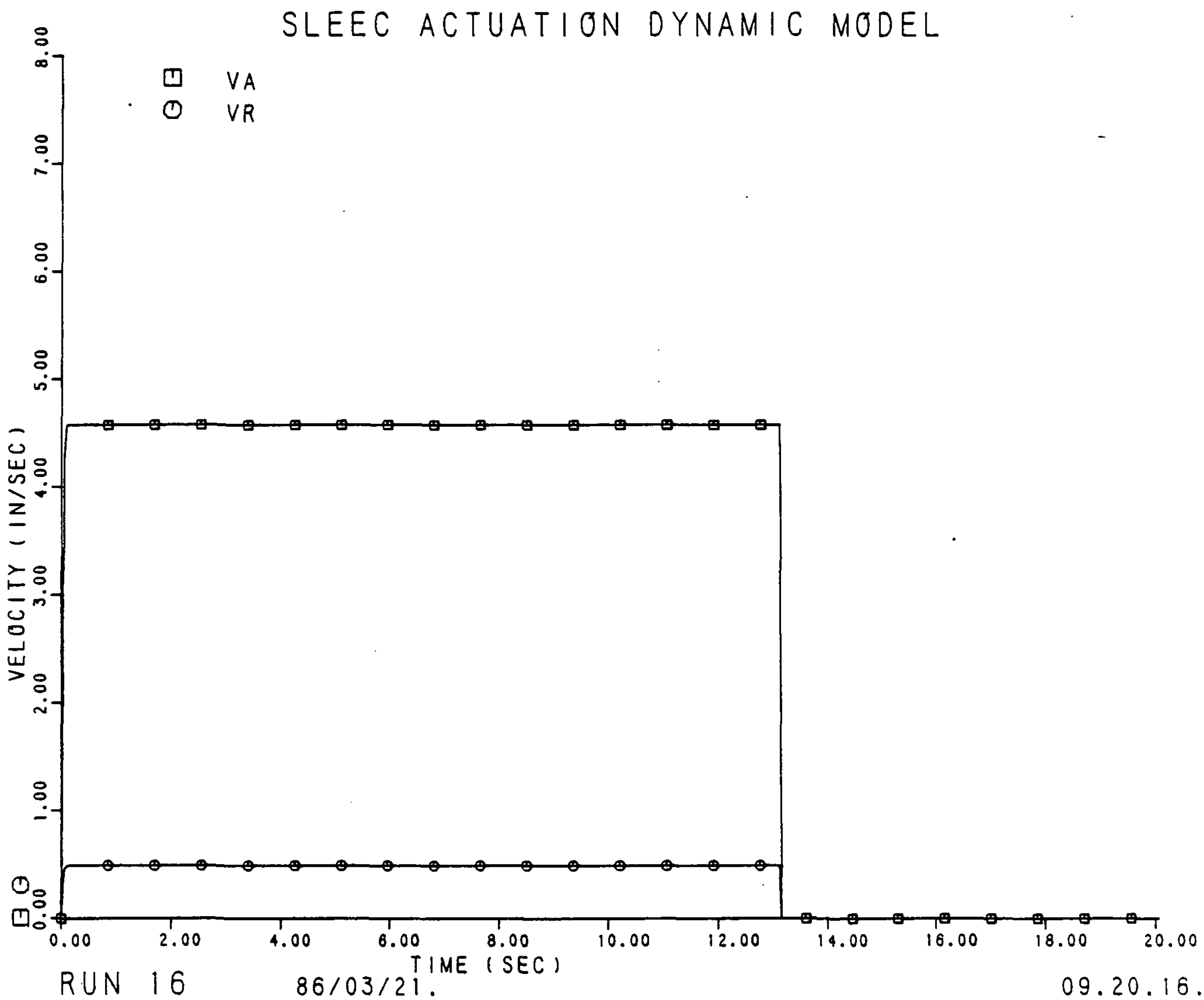

FIGURE 3-7

SLEEC PERFORMANCE SIMULATION OF AXIAL
AND RADIAL VELOCITY FOR MAXIMUM FLIGHT LOADS

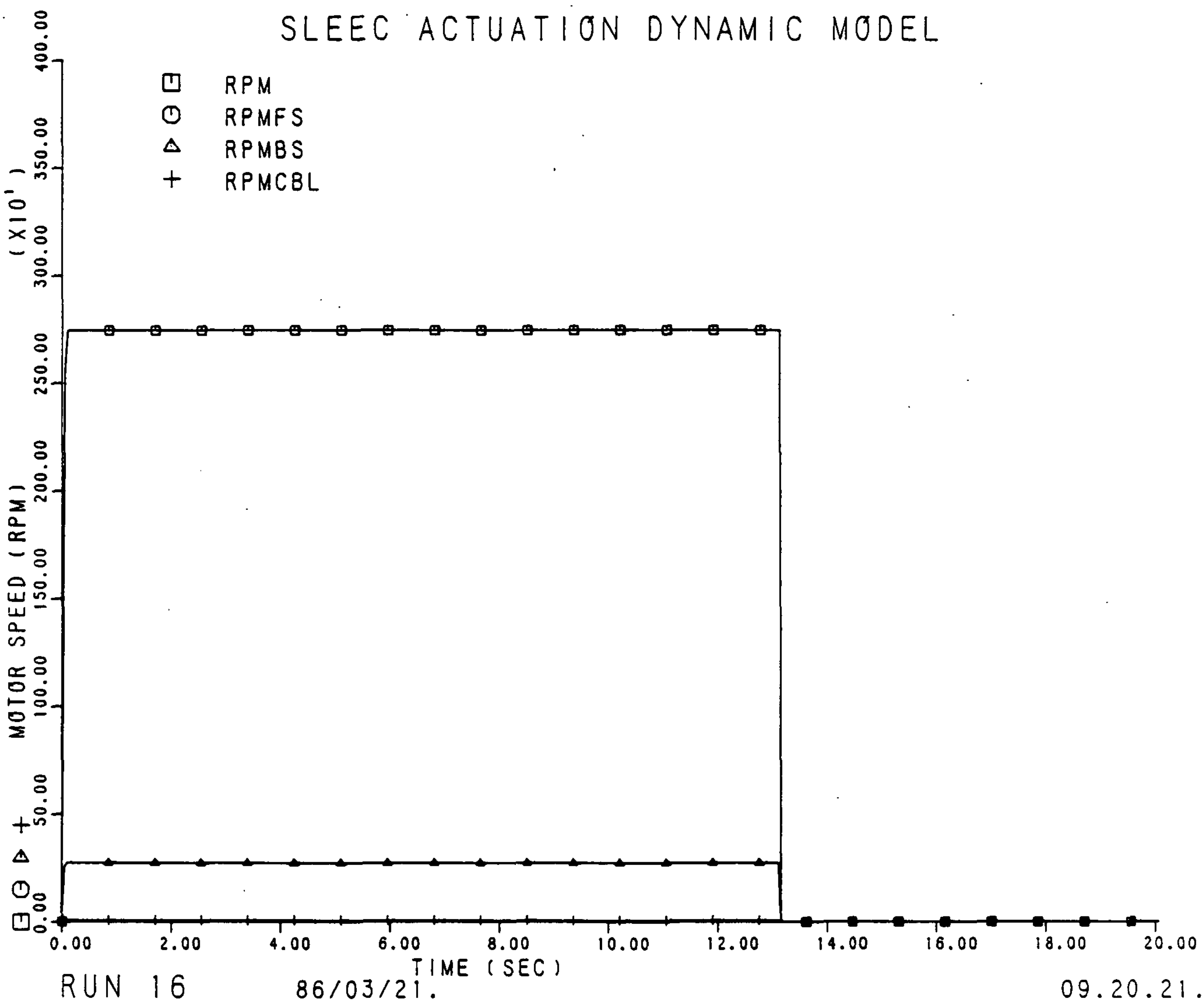

FIGURE 3-8

SLEEC PERFORMANCE SIMULATION OF MOTOR, FLEXSHAFT, BALLSCREW, AND CABLE DRUM SPEEDS FOR MAXIMUM FLIGHT LOADS

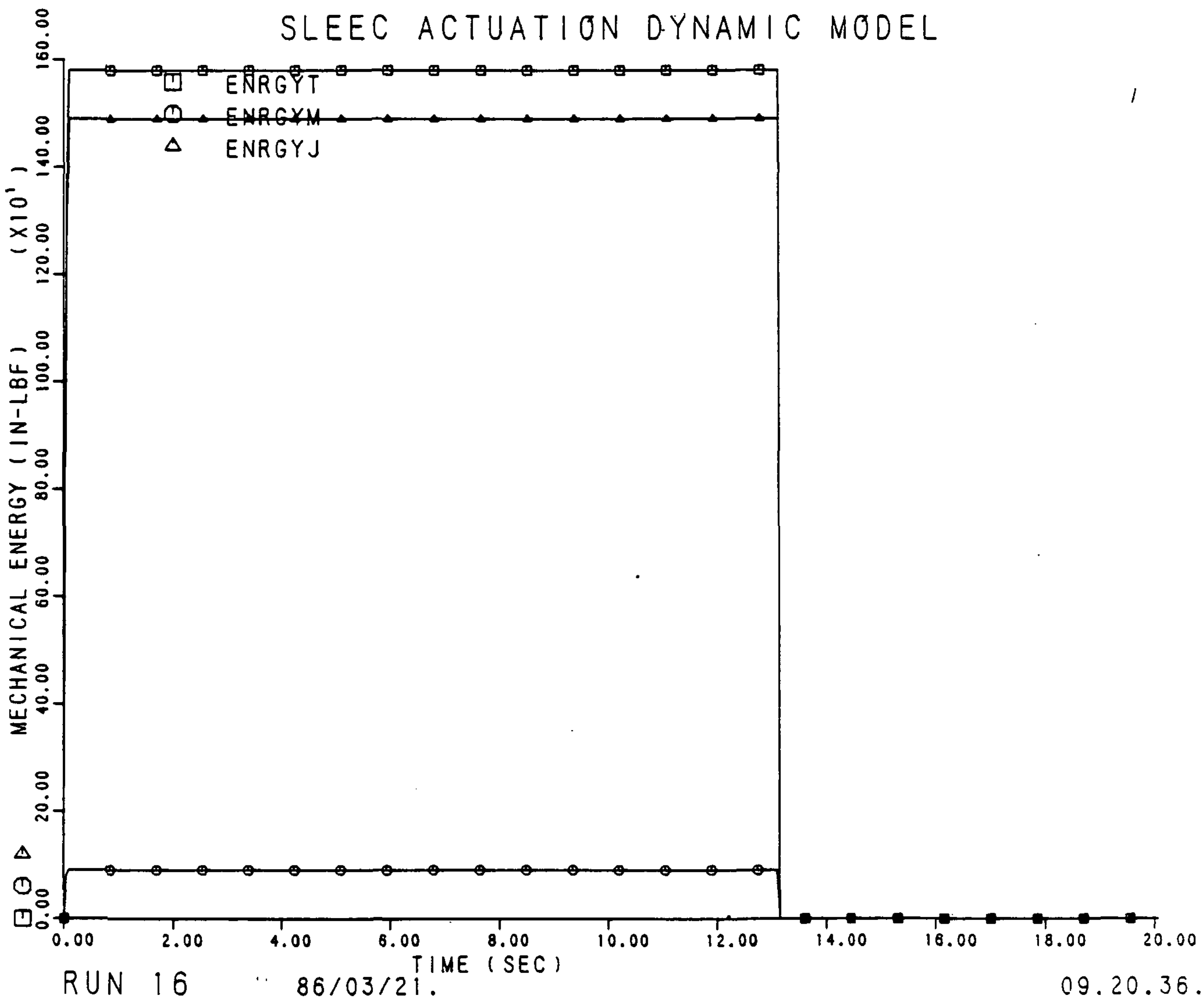

FIGURE 3-9

SLEEC PERFORMANCE SIMULATION OF IMPACT ENERGY
FOR MAXIMUM FLIGHT LOADS

Verification Tests

SECTION 4

VERIFICATION TESTS

4.1 TESTS SUMMARY

The tests defined in this section for the SLEEC actuation system are comprised of three programs. The bench test program, (paragraph 4.2) will verify the design concept; the development test program, (paragraph 4.3) will verify the performance of the SLEEC systems including the actuation system and the shingles; and the acceptance test program (paragraph 4.4) will verify the performance and integrity of the production actuation system components (see Figure 4-1).

4.2 BENCH TESTS

The objective of the bench test program will be to verify the design concept of the SLEEC system by testing a segment of the actuation system at three loading conditions: a nominal load, a maximum load, and 1.4 times the maximum load.

4.2.1 Description of Test Segment

The test segment shall consist of one-sixth of the actuation system, i.e., an axial drive ballscrew, two cable payout drums mounted on a simulated inner shingle, a programmed simulated hoop load achieved through the use of air cylinders attached to each drum cable, and a programmed air cylinder which will simulate one-sixth of the rocket plume load (see Figure 4-2).

4.2.2 Pretest Inspection

A pretest inspection shall specify a review of the piece-part inspection record and note any anomalies in the test logbooks.

4.2.3 Test Equipment and Setup

The test equipment shall consist of the following:

a. A mounting fixture representing one-sixth of the exit cone.

b. An axial load cylinder including a load cell and programmer.

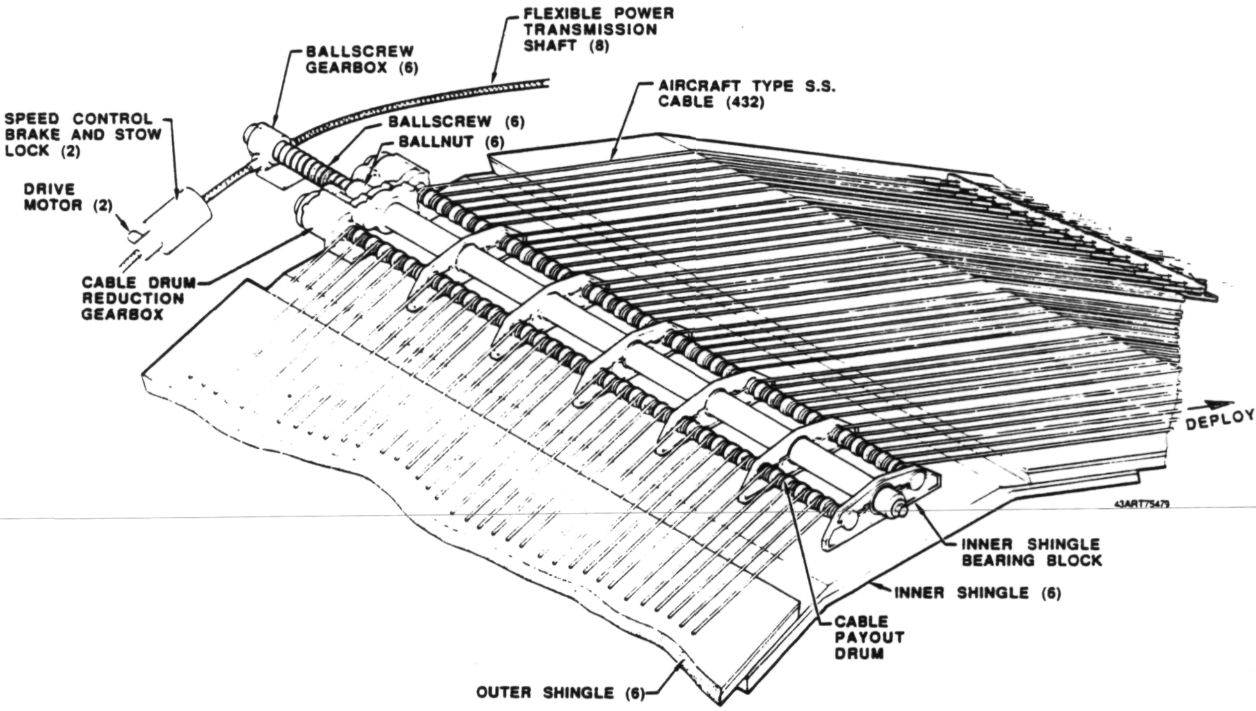

FIGURE 4-1

SLEEC ACTUATION SYSTEM COMPONENTS

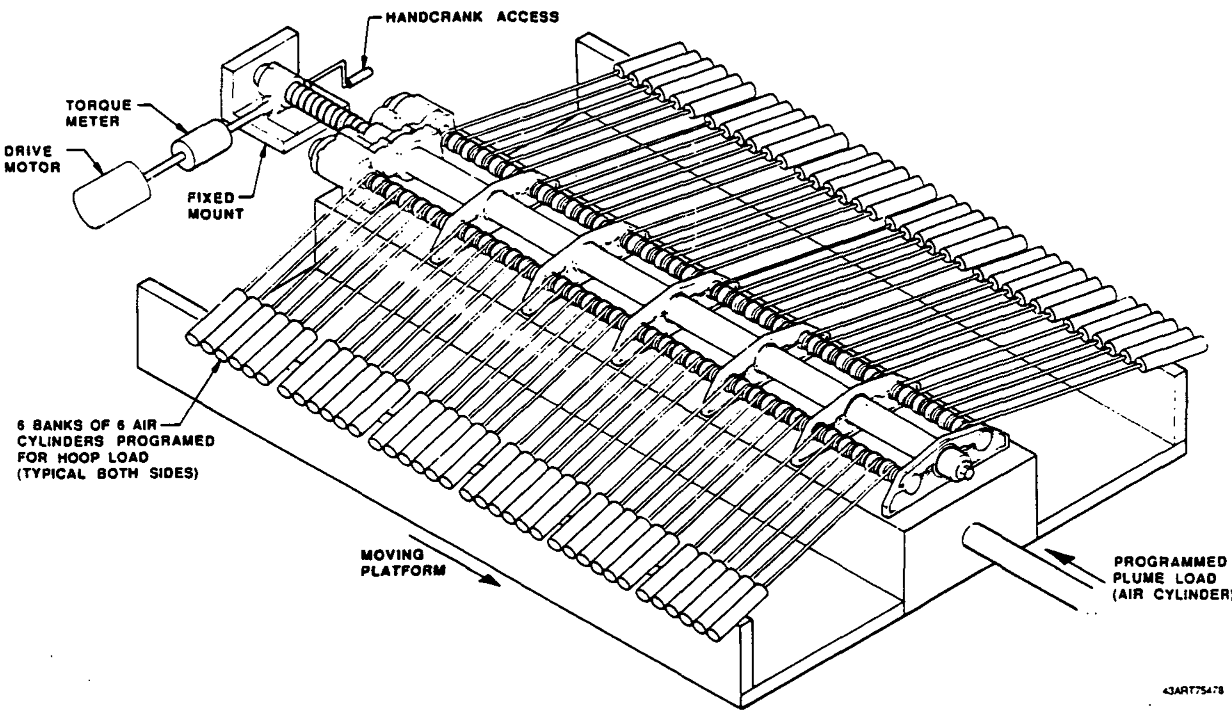

FIGURE 4-2

SLEEC BENCH TEST SETUP

c. 72 load cylinders simulating cable hoop loads with a programmer for cylinder pressure.

d. A torque meter with a flexshaft input.

e. A drive motor with a flexshaft input.

The test setup shall be constructed as shown in Figure 4-2. The following data shall be continuously recorded during deployment of the one-sixth SLEEC segment:

- Hoop load cylinder pressure (0-1500 psi)
- Simulated one-sixth plume load (0-10K lbs)
- Input torque (±50 in-lbs)
- Stroke (0-60 inches)
- Time (0-25 seconds)

4.2.4 Test Conditions

All tests specified herein shall be conducted under prevailing laboratory ambient conditions as follows:

o	Ambient temperature	80 ±40F
o	Ambient pressure	28.8 ±2.0 in Hg, abs
o	Humidity	5 to 80 percent

4.2.5 Logbooks, Photographs, and Video Tapes

A daily logbook shall be kept of all significant activity. Photographs shall be taken of all test setups and of any significant incidents. A video tape shall be made of the initial actuation cycle of each test.

4.2.6 Test Procedure

4.2.6.1 Test Setup Checkout

a. Hand-crank to the fully deployed position with no axial load and only a 5-pound load on each cable.

b. Record the drag load, torque and stroke.

c. Hand-crank to the fully stowed position.

d. Repeat step (a) using the drive motor instead of the hand-crank.

e. Repeat steps (b) and (c) above.

4.2.6.2 Deploy at 80 Percent, 100 Percent, and 140 Percent of Load

Deploy under the following conditions.

a. Set the axial deployment speed to be ±0.5 in/sec (nominal 20-second deploy time).

b. Set the axial load at 13.3 percent of the total rocket plume load (i.e., set at 5.40K lbs)

c. Set the cable hoop load at 80 percent of the maximum total hoop load (i.e., set at 716 lbs per cable).

d. Record the axial load, hoop load cylinder pressure, torque, and stroke versus time.

e. Hand-crank the setup to the fully-stowed position.

f. Repeat steps (a) through (e) above except that the axial load shall be 16.6 percent of the total plume load (i.e., 6.80K lbs) and the cable hoop load shall be 100 percent of total hoop load (i.e., 894 lbs per cable).

g. Repeat steps (a) through (e) above except with a plume load of 23.2 percent of maximum (i.e., 9.44K lbs), and a cable load of 140 percent of maximum (i.e., 1252 lbs per cable).

h. Complete paragraph 4.2.6.3, step (a).

i. Repeat step (f) above ten times.

4.2.6.3 Post-Test Inspection

a. The test unit shall be closely inspected after the 140-percent load test of step (g) of pargraph 4.2.6.2 and compared to its pre-test condition for any evidence of change due to deformation.

b. After completion of all the bench tests, disassemble and reinspect all piece-parts both visually and dimensionally. Review the results with any logbook entries recorded during the pre-test inspections of paragraph 4.2.2.

4.2.7 Test Success Criterion

There shall be no permanent deformation of the test unit or any of its component parts as determined by visual inspection following the tests of paragraph 4.2.6.2.

4.3 DEVELOPMENT TESTS

The objective of the development tests is to verify the performance of the SLEEC system and demonstrate its operation by simulating hoop loading from the shingles. The fixed cone, compliance ring, inner shingles, and outer shingles are to be supplied by ASPC. The actuation system, fixtures and test setup are to be supplied by GPSD. A horizontal, no-load ground checkout will also be demonstrated for the final system checkout prior to actual flight.

4.3.1 Description of Performance and Demonstration Tests

A complete SLEEC system consisting of fixed exit cone, a structural support for the ballscrew gearboxes, six inner shingles with mounting points for the actuation system, six outer shingles with attachment mounting for the hoop cables, and a complete six-ballscrew SLEEC actuation system shall be set up and mounted for deployment as a total system. The system shall be deployed in a vertical orientation, upward and against load devices which will simulate the rocket plume load (thrust and radial hoop loads) as shown in Figure 4-3. The ground checkout will be accomplished in the horizontal position as shown in Figure 4-4. Gas-filled strut cylinders will be added to increase the pre-tension load in the cables if required for full deployment.

4.3.2 Pre-Test Inspection

Carefully inspect all the component parts, the major setup fixtures, and the instrumentation. Prepare a checklist listing component parts by part number with the characteristics or features that must be inspected. Attach the checklist to the test logbook.

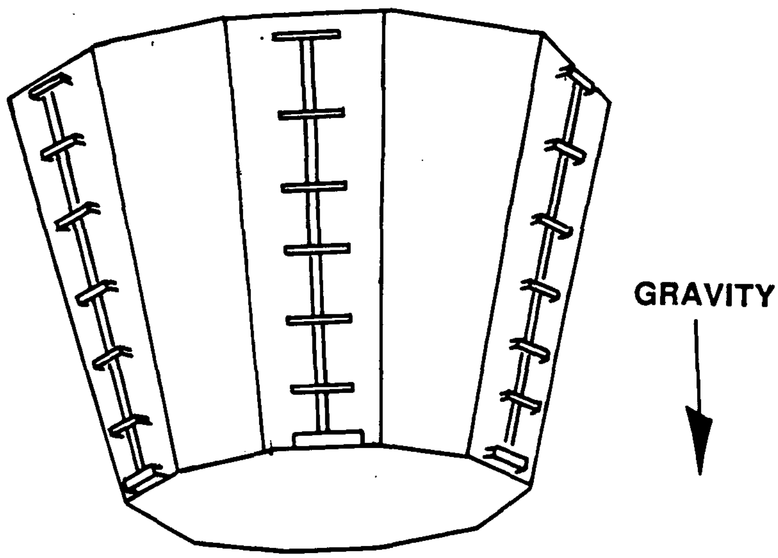

FIGURE 4-3

SLEEC DEVELOPMENT TEST, VERTICAL ORIENTATION

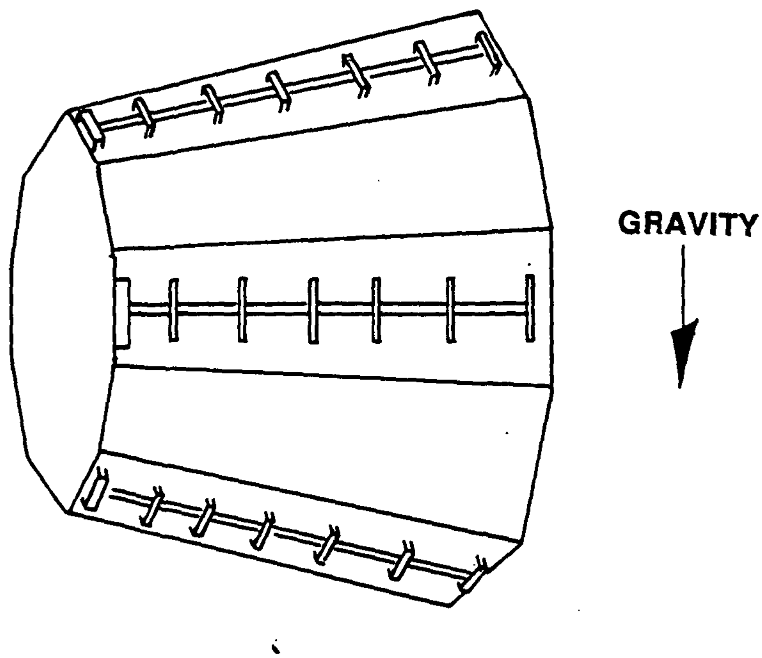

FIGURE 4-4

SLEEC DEVELOPMENT TEST, HORIZONTAL ORIENTATION

4.3.3 Test Equipment and Setup

The test equipment shall consist of the following:

a. A mounting fixture to support the fixed cone

b. A shingle loading mechanism simulating the plume load

c. Six torque meters in the flexshaft loop

d. 36 gas-filled struts simulating shingle loading for the ground checkout

4.3.4 Flight Loading Demonstration

The flight loading demonstration test system shall be setup as in paragraph 4.3.1. It will have six ballscrew stations, each similar to that of Figure 4-1, and arranged as shown in Figure 4-3.

The following data shall be continuously recorded during deployment of the SLEEC:

- Six torques (±50 in-lbs)
- Stroke (0-60 inches)
- Time (0-25 seconds)

4.3.5 Ground Checkout Demonstration

The ground checkout demonstration test assembly shall be set up in a stowed horizontal position. Install the gas-filled struts to retain the orientation of the shingles and maintain the cable tension load during a full deployment. Other than the horizontal orientation, the assembly shall be the same as for the flight loading demonstration, less the shingle loading mechanism (plume load) as shown in Figure 4-4.

The following data shall be continuously recorded during checkout deployment of the SLEEC.

- Six torques (±50 inch-lbs)
- Stroke (0-60 inches)
- Time (0-25 seconds)

4.3.6 Test Conditions

All tests specified herein shall be conducted under prevailing laboratory ambient conditions.

4.3.7 Logbooks, Photographs, and Video Tapes

A daily logbook shall be kept documenting all significant activity. Photographs shall be taken of all test setups and of any significant incidents. A video tape shall be made of the initial actuation cycle of each test.

4.3.8 Test Procedures

4.3.8.1 Test Setup Checkout

With the system setup as described in paragraph 4.3.4 proceed as follows:

a. Hand-crank the setup to the fully-deployed position.

b. Monitor the shingle loading mechanism loading indicators for proper loading over the total stroke of the system. Any imbalance in the six torque readings will indicate system binding or uneven loading from the shingle loading mechanism.

c. Hand-crank the setup to the fully-stowed position.

4.3.8.2 Deploy at 20 Seconds, 10 Seconds and Freerun

a. Deploy the system at 3 ±0.05 in/sec (nominal 20-second deployment time). Repeat paragraph 4.3.8.1 and examine the hardware and data.

b. Deploy the system at 6 ±0.5 in/sec (nominal 10-second deployment time). Repeat paragraph 4.3.8.1 and examine the hardware and data.

c. Disconnect the speed control feedback and fully deploy the system at the freerun speed. Check the system hardware and data.

4.3.8.3 Ground Checkout Demonstration

With the system setup as described in paragraph 4.3.5

a. Hand-crank slowly to deploy fully while observing the action of the shingles. While some out of roundness of the SLEEC due to gravity is permissible for ground checkout, no shingle separation should occur. The gas-filled struts may be progressively removed as long as the shingles maintain their proper relationship to each other. It is desirable to perform the ground checkout with a minimum of gas struts. Monitor the torque readings with each hand-crank checkout.

b. Hand-crank the system into the stowed position while monitoring the shingle and actuation system for abnormalities.

c. Deploy the system with the system drive motor. Monitor the torques versus stroke and the shingle orientation.

4.4 ACCEPTANCE TESTS

An acceptance test will be conducted on each component prior to shipment. It is not practical, nor meaningful, to test the actuation system as an assembly at GPSD's facility. The final acceptance test of the total SLEEC system is best accomplished during final assembly on the SRB. For demonstration of the final assembly checkout see paragraph 4.3.5. The components which will be individually acceptance tested are the:

- Actuation assembly (six required per system).
- Drive motor/brake assembly (two required per assembly).
- Flexshaft assembly, actuator to actuator (four required per assembly).
- Flexshaft assembly, motor/brake to actuator (four required per assembly).

4.4.1 Actuation Assembly Acceptance Test Procedure

4.4.1.1 Description of Test Setup

The actuation assembly shall be mounted on a simulated inner shingle (also used for shipping the assembly) and installed in the test fixture shown in Figure 4-5.

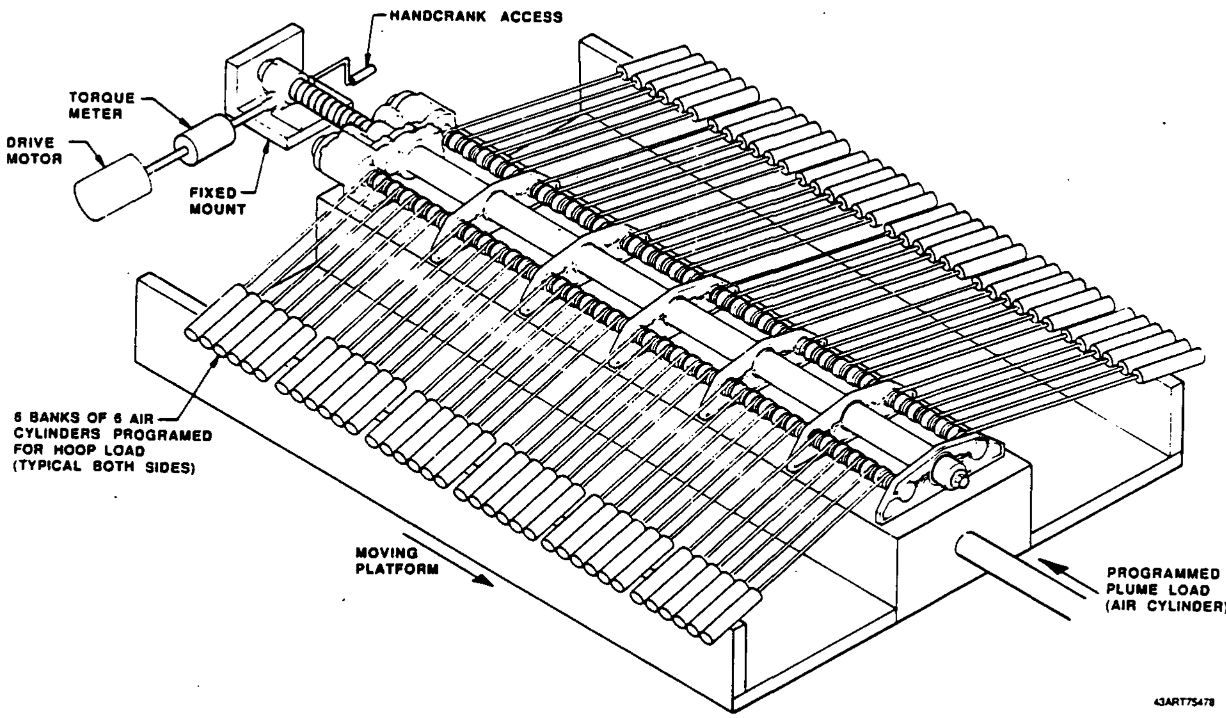

FIGURE 4-5

SLEEC ACCEPTANCE TEST SETUP

4.4.1.2 Pre-Test Inspection

Visually examine the hardware and review all documentation prior to the start of the test.

4.4.1.3 Test Equipment and Setup

The test equipment shall consist of the following:

a. A mounting fixture (simulated one-sixth SLEEC).

b. An axial load cylinder (with load cell and programmer).

c. 72 load cylinders (cable hoop loads).

d. A torque meter (flexshaft input).

e. A drive motor (flexshaft input).

The test setup shall be constructed in accordance with Figure 4-5.

4.4.1.4 Test Data

The following data shall be continuously recorded during deployment of the actuation assembly.

- Load cylinder pressure (0-1500 psi)
- Simulated one-sixth plume load (0-10K lbs)
- Input torque (±50 inch-lbs)
- Stroke (0-60 inches)
- Time (0-25 seconds)

4.4.1.5 Test Conditions

All tests specified herein shall be conducted under prevailing laboratory ambient conditions.

4.4.1.6 Test Procedure

4.4.1.6.1 Hand-crank Test

a. Hand-crank the assembly to fully deploy with no axial load and a 5-pound load per cable.

b. Record the drag load, torque, and stroke.

c. Return the actuator to the stowed position by hand-cranking.

4.4.1.6.2 Normal Maximum Deployment Test

a. Deploy the assembly at 4 ±0.5 in/sec (nominal 13-second deployment time).

b. Set the axial programmed load at 6,800 pounds maximum and set the cable programmed load at 890 pounds per cable maximum.

c. Record the axial load, cable loading, cylinder pressure, torque, and stroke versus time.

4.4.1.6.3 Acceptance Criteria

a. There shall be no permanent deformation of the test unit or any of its component parts as determined by visual inspection.

b. All test data shall be within the tolerances of paragraph 4.4.1.4.

c. The operation cycle shall be complete, smooth and without any hesitation.

4.4.2 Drive Motor/Brake Assembly ATP

The acceptance test for this assembly will consist of a simulated overhauling loads test in order to confirm the speed control function. In addition, a simulated stiction test will be developed to verify the drive motor function.

4.4.3 Flexshaft Assembly ATP

ATPs for flexshafts have been well established from aircraft thrust reverser applications. The Garrett Engineering Test Instructions TI-3237564 attached at the end of this section contain instructions for testing the Flexshaft Assembly for the Peacekeeper Stage II Extendible Nozzle Exit Cone (ENEC) and are presented herein as an example of an established application and procedure.

GARRETT PNEUMATIC SYSTEMS DIVISION
A DIVISION OF THE GARRETT CORPORATION
PHOENIX, ARIZONA

ENGINEERING
TEST INSTRUCTIONS

PREPARED BY	ORIGINAL ISSUE DATE	TI-	REV.	PAGES
R. P. Austen	10-4-84	3237564	NC	2

APPROVED BY	LAB REVIEW BY	ATTACHMENTS
J. W. Merritt/CGT	A. Glenn	DS-3237564-1 SK1 DS-3237564-2
TEST LOCATION: Receiving Inspection		

TITLE
FLEXIBLE SHAFT ASSEMBLY 3237564-1,-2

REV.	EFFECTIVITY DATE (CR NO.)	PAGES AFFECTED	REFERENCES	DESCRIPTION OF CHANGE
NC	10-4-84		ATP-3237564 dated 9-7-84.	Initial Issue.

1. INTRODUCTION

1.1 Purpose - These instructions outline the testing procedures to be performed upon the subject unit. Any unit failing to meet the specified requirements shall be rejected.

2. PROCEDURE

NOTES: 1. Do not deviate from the given sequence of this procedure.

2. Any torque applied shall be quickly released after obtaining the required value. The torque wrench shall be removed to read the original position (refer to SK1 for proper procedure).

The shaft shall be equalized before and after each test by performing the following:

- Install the unit in the test fixture T-198514 or equivalent.
- Select the proper fittings for shaft size.
- Layout the shaft assembly in a straight line.
- Support the end flanges and the casing at approximately 12 inch intervals.
- Lock one end of the core to prevent rotation and apply torque loads in the following manner:

150 in.-lb clockwise and counterclockwise
100 in.-lb clockwise and counterclockwise
50 in.-lb clockwise and counterclockwise
25 in.-lb clockwise and counterclockwise
10 in.-lb clockwise and counterclockwise
5 in.-lb clockwise and counterclockwise

2.1 Proof Load Tests

2.1.1 Apply a proof load test torque of 290 ±5 lb-in. in the clockwise direction. The free end of the shaft shall return to the original position within ±10 degrees.

2.1.2 Repeat paragraph 2.1.1 applying the torque in the counterclockwise direction.

2.2 <u>Angular Deflection</u> Apply a torque of 100 ±5 lb-in. to the free end of the shaft in a clockwise direction. The angular deflection shall be within the limits shown below per applicable dash number. Remove the torque from the shaft; the free end of the shaft shall return to the original position within ±5 degrees.

Dash No.	Maximum Angular Deflection deg
-1	72
-2	31

2.2. Repeat paragraph 2.2 applying the torque in the counter-clockwise direction.

TI-1301-1*

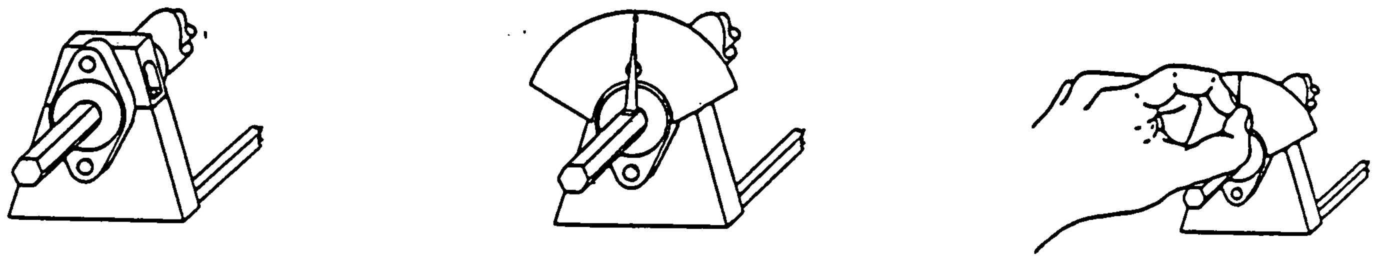

STEP A: INSTALL THE UNIT AS DESCRIBED IN THE TEXT
AFTER EQALIZATION, ZERO THE INDICATOR.

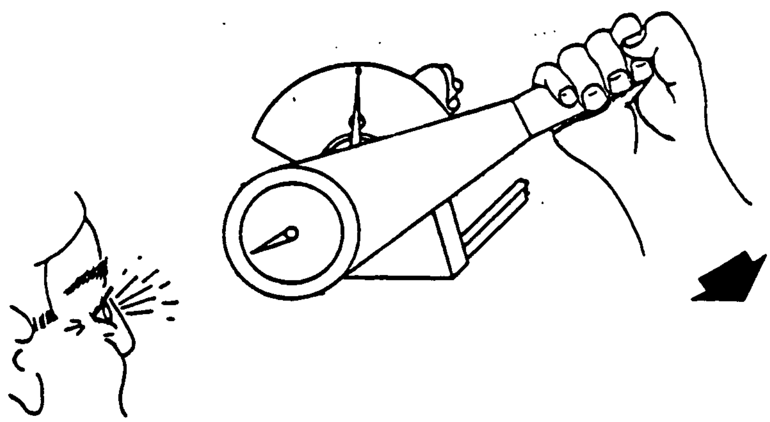

STEP B: INSTALL TORQUEMETER AND APPLY TORQUE AS PRESCRIBED IN THE TEXT, OBSERVE TORQUE.

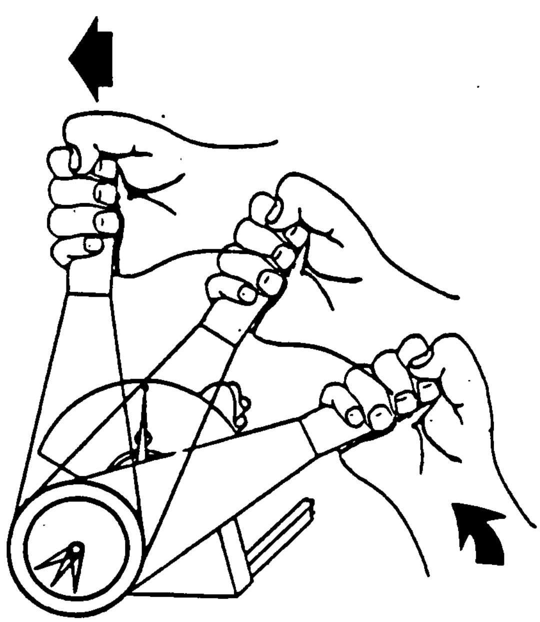

STEP C: SWIFTLY BUT SMOOTHLY
REMOVE THE TORQUE WITHOUT OVERSHOOT.
(DO NOT PASS ZERO ON PROTRACTOR)

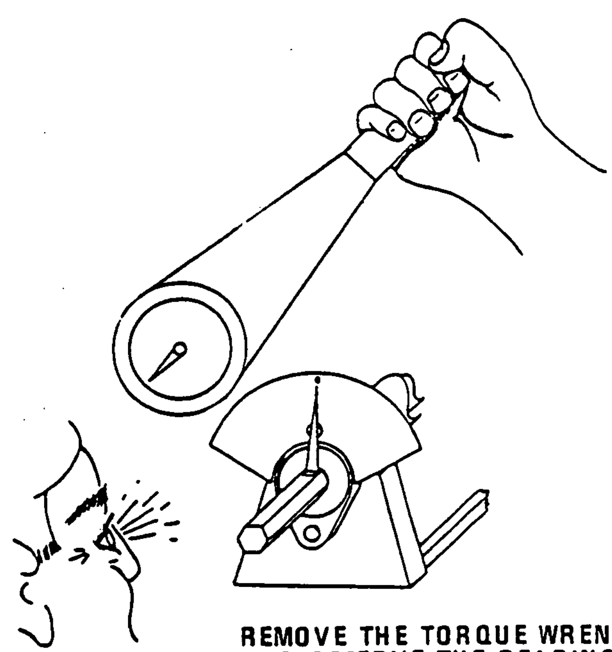

STEP D: REMOVE THE TORQUE WRENCH
AND OBSERVE THE READING
ON THE PROTRACTOR

TORQUE PROCEDURE

GARRETT PNEUMATIC SYSTEMS DIVISION
A DIVISION OF THE GARRETT CORPORATION
PHOENIX ARIZONA

Test Date__________

ATP-3237564, Rev.____

TI-3237564, Rev.____

Instrumentation Accept ____

DS-3237564-2

GARRETT PART 3237564-2

TESTED BY____________________ STATION NO. ________________

Unit S/N	Proof (MC)* Accept CW CCW	Return ±10 deg Actual CW CCW	Angular Deflection CW 31 deg Max Deflection Actual	Angular Deflection CW Springback ±5 degrees Actual	Angular Deflection CCW 31 deg Max Deflection Actual	Angular Deflection CCW Springback ±5 degrees Actual	Unit Accept

*(MC) denotes major characteristics defined in GPSD Report 41-3803.

GARRETT PNEUMATIC SYSTEMS DIVISION
A DIVISION OF THE GARRETT CORPORATION
PHOENIX ARIZONA

Test Date__________

ATP-3237564, Rev._____

TI-3237564, Rev._____

Instrumentation Accept _____

DS-3237564-1

GARRETT PART 3237564-1

TESTED BY____________________

STATION NO. ____________________

Unit S/N	Proof (MC)* Accept CW CCW	Return ±10 deg Actual CW CCW	Angular Deflection CW 72 deg Max Deflection Actual	Angular Deflection CW Springback ±5 degrees Actual	Angular Deflection CCW 72 deg Max Deflection Actual	Angular Deflection CCW Springback ±5 degrees Actual	Unit Accept

*(MC) denotes major characteristics defined in GPSD Report 41-3803.

Loads and Stress Analysis

SECTION 5

LOADS AND STRESS ANALYSIS

5.1 DESIGN LOAD SUMMARY

Figure 5-1 shows the internal pressure distribution which was used to calculate the resultant forces acting on the SLEEC shingles. It is the piecewise linear approximation of the actual, continually-varying pressure.

The pressure-induced components of force acting in the axial and radial directions were determined for both inner and outer shingles for the fully extended position with the assumption that external pressure equaled zero (maximum load at vacuum conditions).

For the inner shingle:

Radial F_x = 19,218 lb

Axial F_z = 4,085 lb

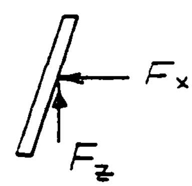

For the outer shingle:

Radial F_x = 25,434 lb

Axial F_z = 5,406 lb

These forces <u>include</u> a safety factor of 1.4. The outer shingle overlaps the inner shingle by approximately 3 inches in a strip extending the length of the shingle. In calculating outer shingle forces, this overlap area was omitted. The total axial resultant force on the complete cone is then:

$$F_{z_{total}} = 6(4085 + 5406) = 56,946 \text{ lb.}$$

The detailed shingle load calculations are shown in paragraph 5.4 of this document.

Figures 5-2 and 5-3 show free bodies of the outer and inner shingles. The significant forces acting on the shingles are the ball screw thrust force

$$F_B = 9,702 \text{ lb,}$$

and the resultant cable (hoop) tensile force

$$F_h = 45,106 \text{ lb.}$$

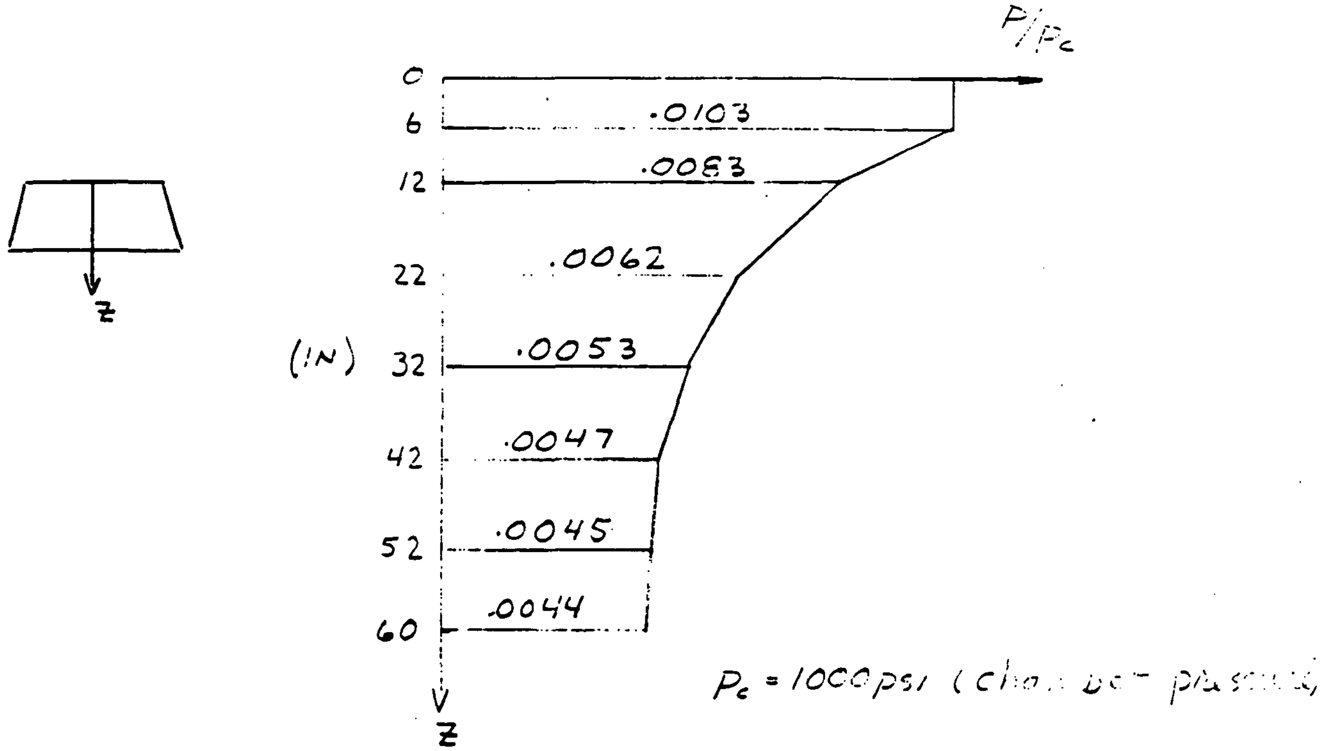

FIGURE 5-1

NOZZLE PRESSURE DISTRIBUTION USED
TO CALCULATE RESULTANT FORCES

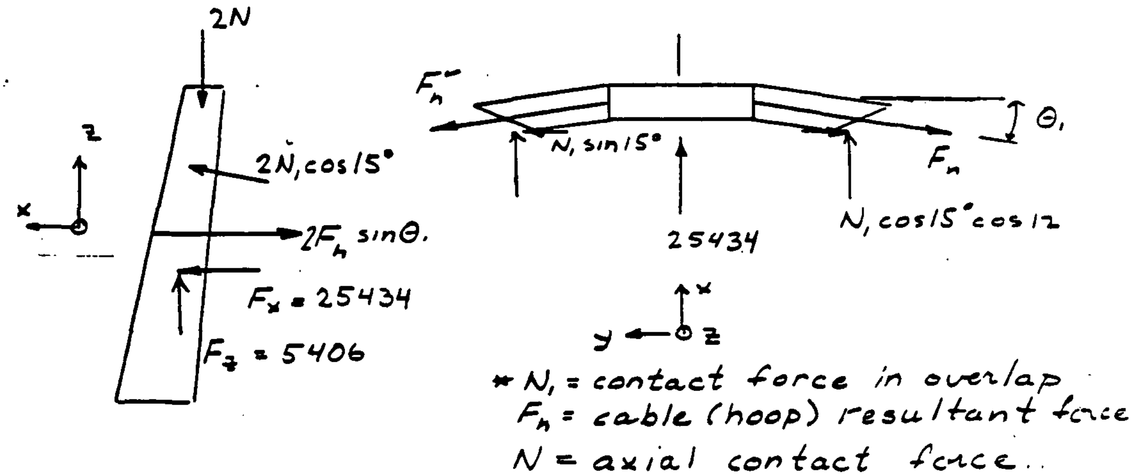

FIGURE 5-2

OUTER SHINGLE FREEBODY

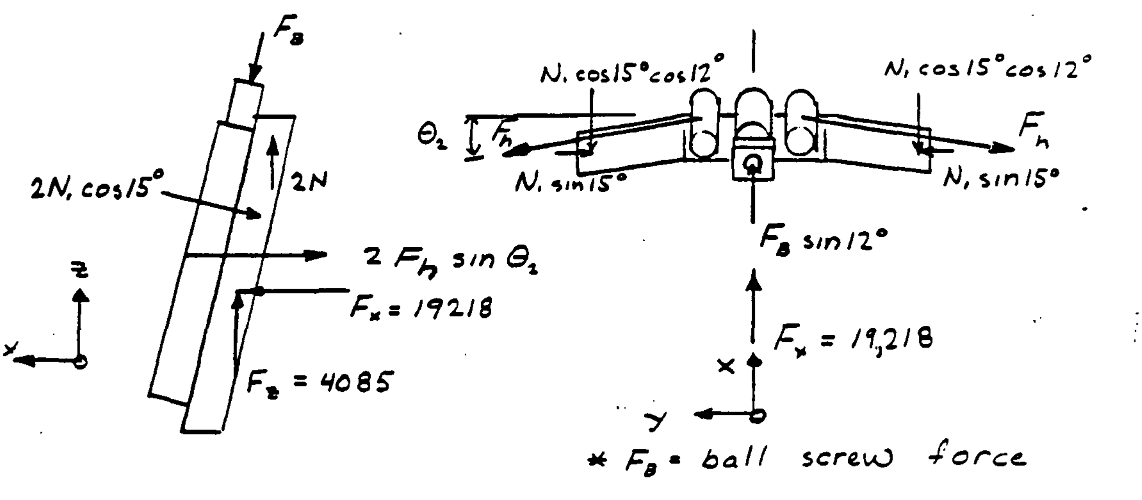

FIGURE 5-3

INNER SHINGLE FREEBODY

Note that since the radial outward pressure resultant on the outer shingle is greater than that on the inner shingle (the inner shingle is smaller) the hoop tension resultant (cable) must make a slightly shallower angle with the normal to the inner shingle centerline than to that of the outer shingle in order that the shingles be pressed together

$$\theta_2 > \theta_1 .$$

Calculations show (see paragraph 5.6) that if

$$\theta_1 = 13^\circ,$$

and

$$\theta_2 = 17^\circ,$$

(the sum of these angles is 30 degrees which is the angle between shingle centerlines) then a contact force,

$$N_1 = 498 \text{ lb},$$

exists between the shingles at each overlap. The overlap contact force may be increased by decreasing the angle θ_1 and increasing θ_2 by the same amount. If θ_1 is 12 degrees and θ_2 equals 18 degrees, a normal force of 1,304 pounds exists at the overlap. Hoop tension also increases slightly to 45,141 pounds. These results are required for static equilibrium, assuming the shingles to be rigid bodies. In actual practice, the shingles tend to circumferentially deflect somewhat thereby naturally supplying the cable angularity required for static equilibrium.

The existence of a contact force between the shingles increases the frictional resistance to cone extension, however it provides for a gas seal between the shingles during and subsequent to deployment.

5.2 SLEEC DEPLOYMENT TORQUE

The unique condition which exists in the SLEEC concept of nozzle extension is that the radial component of pressure within the cone tends to expand it and provides the power for extending the system against axial loads. Since the pressure force on the cone moves perpendicularly to its line of action (see Figure 5-4) during deployment, no net work is done; i.e., the negative work of the axial component of pressure is exactly balanced by the positive work of the lateral component of pressure as long as deployment is along the cone angle. This means that, neglecting friction and inertia, cone extension requires no driving torque at all.

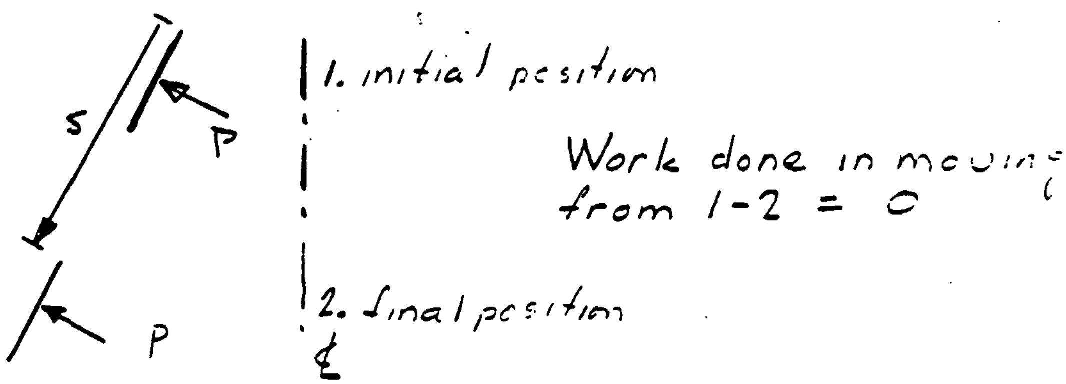

FIGURE 5-4

EXTENSION ALONG THE CONE ANGLE

This conclusion is verified by the determination of the torques acting on the ballscrew in paragraph 5.7. The torque on the ballscrew due to the ballscrew thrust (9,702 lb) is

$$T_B = 1,544 \text{ in-lb.}$$

The torque acting on one cable drum due to hoop tension (45,106 lb) is

$$T_h = 29,590 \text{ in-lb.}$$

The gear reduction from the cable drum to the ballscrew guide is derived in paragraph 5.5 which defines the kinematics of deployment. The reduction ratio is 38.3:1 so that the torque on the ballscrew guide due to cable roller torque is then

$$T_B = \frac{29590}{38.3} = 772 \text{ in-lb.}$$

The other cable drum provides an additional 772 in-lb so that a total of 1,544 in-lb is transmitted through the splined shaft to the ballscrew, exactly balancing the thrust torque. No driving torque, then, is necessary to maintain cone equilibrium. Since the ratio between the axial and radial components is constant throughout the stroke, the torque equilibrium for the ballscrew exists throughout deployment. In reality, if friction loads are small, a brake is necessary to prevent the system from deploying due to the 1-g weight force.

5.3 COMPONENT CRITICAL LOAD AND STRESS SUMMARY

The results of the component load and stress analysis are summarized in Table 5-1. The detailed analyses are given in paragraphs 5-7 and 5-8. The two most critical items are the axial ballscrew and the cable drum. The Euler buckling force of the axial ballscrew is 15,394 pounds compared to an applied force of 9,702 pounds. The resulting margin of safety is 0.537. The cable drum must resist the torque due to the resulting hoop tension of 45,106 pounds acting on a pitch radius of 0.656 inches resulting in a peak torsional shear stress of 105,842 psi. It is proposed to use AISI S7 tool steel to fabricate the drums. The material properties of this material are

Ultimate tensile strength, $F_{T_u} = 275$ ksi

Yield tensile strength, $F_{T_y} = 205$ ksi

Elongation (2-in gage), e = 10%

The torsional shear yield stress is assumed to be 0.6 times the tensile yield stress or

$$F_{s_y} = 123 \text{ ksi},$$

resulting in a margin of safety of 0.162. All critical components show positive margins of safety for the design loads. This provides verification that the SLEEC actuation system is structurally adequate to withstand the fully-deployed pressure loads.

TABLE 5-1

CRITICAL COMPONENT LOAD AND STRESS SUMMARY
(BASED ON A SAFETY FACTOR OF 1.4)

Component	Critical Load	Critical Stress	Allowable Value	Margin of Safety
Flex cable	Braking torque 220 in-lb	-	Proof torque 350 in-lb	0.591
Ballscrew	Axial compression 9,702 lb	-	Buckling load 15,394 lb	0.587
	Torque 1,545 in-lb	Negligible	Shear stress 52,000 psi	large
Spline shaft	Torque 1,545 in-lb	Shear stress 13,276 psi	Shear stress 52,000 psi	large
Cable drum	Torque 29,590 in-lb	Shear stress 105,842 psi	Shear stress 123,000 psi	0.162
	Bending moment 12,892 in-lb	Bending stress 92,224 psi	Bending stress 205,000 psi	1.223
	Combined bending 12,892 in-lb, and torque 22,665 in-lb	Shear stress 93,267 psi	Shear stress 123,000 psi	0.319
Cable	Tension 1,790 lb	-	Tension 3700 lb	1.07
Main mounting bracket	Gear box torque reaction 28,888 in-lb	Bending stress 27,182 psi	Bending stress 90,000 psi	2.30
	Ballscrew thrust moment	Bending stress 49,480 psi	Bending stress 90,000 psi	0.819

5.4 Calculation of Individual Shingle Loads

5.4.1 OUTER SHINGLE LOADS

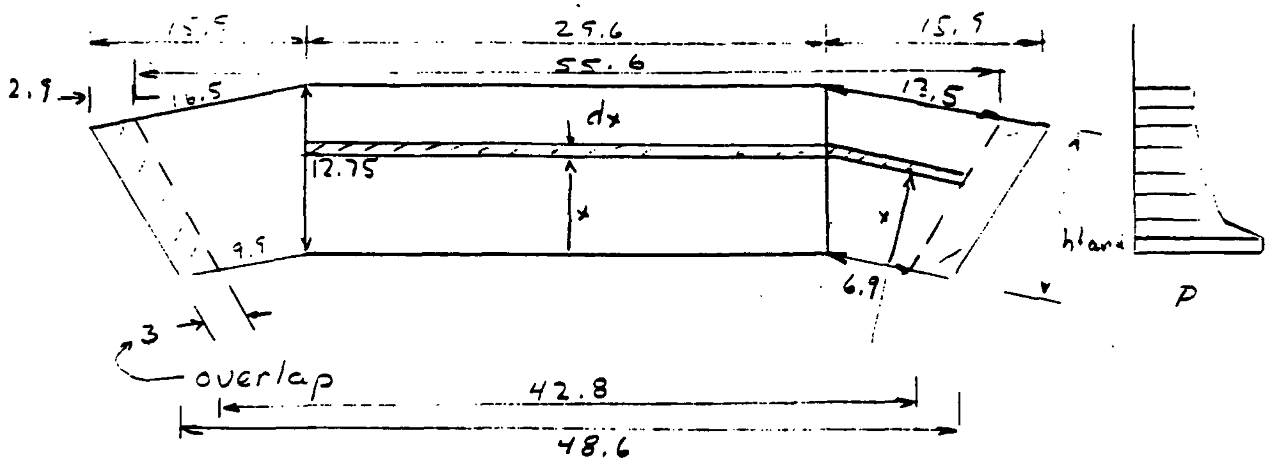

FIGURE 5-5

PROJECTED AREA OF OUTER SHINGLE FOR AXIAL RESULTANT

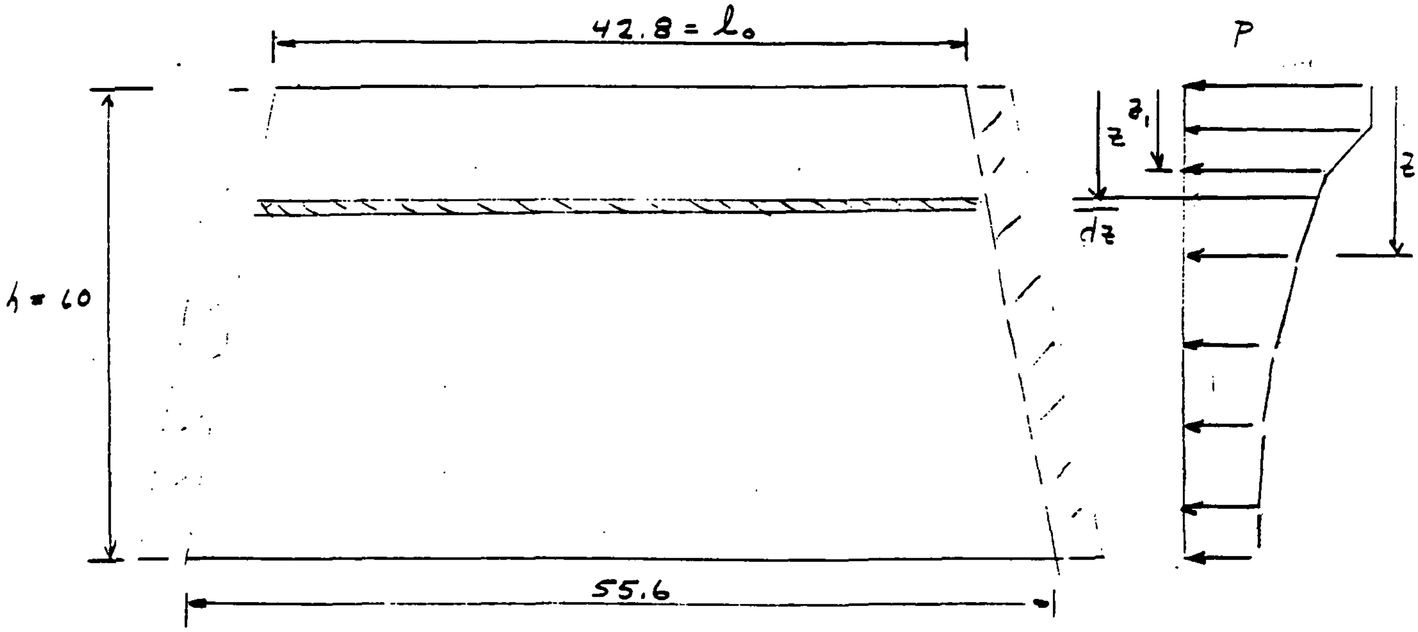

FIGURE 5-6

PROJECTED AREA OF OUTER SHINGLE FOR HORIZONTAL (RADIAL) RESULTANT

5.4.1.1 Horizontal (Radial) Force (F_x) on Outer Shingle

Break the pressure into linearly varying segments

$$\ell = \ell_o + \frac{\Delta \ell}{h} z$$

$$p = p_1 - \frac{\Delta p}{\Delta z}(z - z_1) = \left(p_1 + \frac{\Delta p}{\Delta z} z_1\right) - \frac{\Delta p}{\Delta z} z$$

$$d(\Delta F_x) = p\ell\, dz = \left(\ell_o + \frac{\Delta \ell}{h} z\right)\left[\left(p_1 + \frac{\Delta p}{\Delta z} z_1\right) - \frac{\Delta p}{\Delta z} z\right] dz$$

$$= \left\{\ell_o\left(p_1 + \frac{\Delta p}{\Delta z} z_1\right) + \left[\left(p_1 + \frac{\Delta p}{\Delta z} z_1\right)\frac{\Delta \ell}{h} - \ell_o \frac{\Delta p}{\Delta z}\right] z - \frac{\Delta \ell}{h}\frac{\Delta p}{\Delta z} z^2\right\} dz$$

$$\Delta F_x = \ell_o\left(p_1 + \frac{\Delta p}{\Delta z} z_1\right)(z_2 - z_1) + \left[\left(p_1 + \frac{\Delta p}{\Delta z} z_1\right)\frac{\Delta \ell}{h} - \ell_o \frac{\Delta p}{\Delta z}\right]\left(\frac{z_2^2 - z_1^2}{2}\right) - \frac{\Delta \ell}{h}\frac{\Delta p}{\Delta z}\left(\frac{z_2^3 - z_1^3}{3}\right)$$

$\ell_o = 42.8$
$\Delta \ell = 55.6 - 42.8 = 12.8$
$h = 60$
$z_2 = 6$
$z_1 = 0$
$\Delta p = 0$
$p_1 = .0103\, p_c$

$$\Delta F_{x_1} = p_c\left(42.8(.0103)(6) + .0103\left(\frac{12.8}{60}\right)\left(\frac{6^2}{2}\right)\right) = 2.6846\, p_c$$

$z_2 = 12$
$z_1 = 6$
$p_1 = .0103\, p_c$
$\Delta p = .002\, p_c$
$\Delta z = 6$

$$\Delta F_{x_2} \quad P_c\left((42.8)\left[.0103 + \frac{.002}{6}(6)\right](6) + \left[(.0123)\frac{12.8}{60} - 42.8\left(\frac{.002}{6}\right)\right]\left(\frac{12^2-6^2}{2}\right) - \frac{12.8}{60}\,\frac{.002}{6}\left(\frac{12^3-6^3}{3}\right)\right) = 2.4941\,P_c$$

$z_2 = 22$

$z_1 = 12$

$p_1 = .0083$

$\Delta p = .0021$

$\Delta z = 10$

$$\Delta F_{x_3} = P_c\left(42.8\left[.0083 + \frac{.0021}{10}(12)\right]10 + \left\{\left[\quad\right]\frac{12.8}{60} - 42.8\left(\frac{.0021}{10}\right)\right\}\left(\frac{22^2-12^2}{2}\right) - \frac{12.8}{60}\,\frac{.0021}{10}\left(\frac{22^3-12^3}{3}\right)\right) = 3.3622\,P_c$$

$z_2 = 32$

$z_1 = 22$

$p_1 = .0062$

$\Delta p = .0009$

$\Delta z = 10$

$$\Delta F_{x_4} = P_c\left(42.8\left[.0062 + \frac{.0009}{10}(22)\right]10 + \left\{\left[\quad\right]\frac{12.8}{60} - 42.8\left(\frac{.0009}{10}\right)\right\}\left(\frac{32^2-22^2}{2}\right) - \frac{12.8}{60}\left(\frac{.0009}{10}\right)\left(\frac{32^3-22^3}{3}\right)\right) = 2.7906\,P_c$$

$z_2 = 42$

$z_1 = 32$

$p_1 = .0053$

$\Delta p = .0006$

$\Delta z = 10$

$$\Delta F_{x_5} = P_c\left(42.8\left[.0053 + .0006\left(\frac{32}{10}\right)\right]10 + \left\{\left[\quad\right]\frac{12.8}{60} - \frac{42.8}{10}(.0006)\right\}\left(\frac{42^2-32^2}{2}\right) - \frac{12.8}{60}\left(\frac{.0006}{10}\right)\left(\frac{42^3-32^3}{3}\right)\right) = 2.5336\,P_c$$

$z_2 = 52$
$z_1 = 42$
$p_1 = .0047$
$\Delta p = .0002$
$\Delta z = 10$

$$\Delta F_{x_6} = p_c \Big| 42.8[.0047 + .0002(4.2)]10 + \{ (\quad] \frac{12.8}{60} - 4.28(.0002)\} \left(\frac{52^2 - 42^2}{2}\right) - \frac{12.8}{60}\left(\frac{.0002}{10}\right)\left(\frac{52^3 - 42^3}{3}\right) \Big| = 2.3531\, p_c$$

$z_2 = 60$
$z_1 = 52$
$p_1 = .0045$
$\Delta p = .0001$

$$\Delta F_{x_7} = p_c \Big| 42.8[.0045 + .0001\frac{(52)}{8}]8 + \{[\quad] \frac{12.8}{60} - 42.8\left(\frac{.0001}{8}\right)\} \left(\frac{60^2 - 52^2}{2}\right) - \frac{128}{60}\left(\frac{.0001}{8}\right)\left(\frac{60^3 - 52^3}{3}\right) \Big| = 1.9489\, p_c$$

$F_x = (2.6846 + 2.4941 + 3.3622 + 2.7906 + 2.5336 + 2.3531 + 1.9489)\, p$
$p_c = 1000$ psi (chamber pressure
$F_x = 18.167\,(1000)$

$F_x = 18,167$ LB

5.4.6.2 Axial Force on outer shingle

$F_z = F_x \tan\alpha = 3862$ LB

5.4.2 INNER SHINGLE LOADS

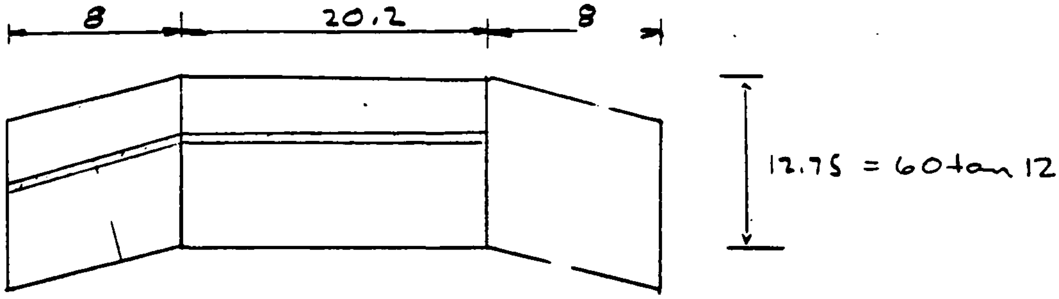

FIGURE 5-7

PROJECTED AREA OF INNER SHINGLE FOR AXIAL RESULTANT

$$F_z = P_{av} A = 6.32[(20.2)(12.75) + 2(8)(12.75)]$$

$$F_z = 2917 \text{ LB}$$

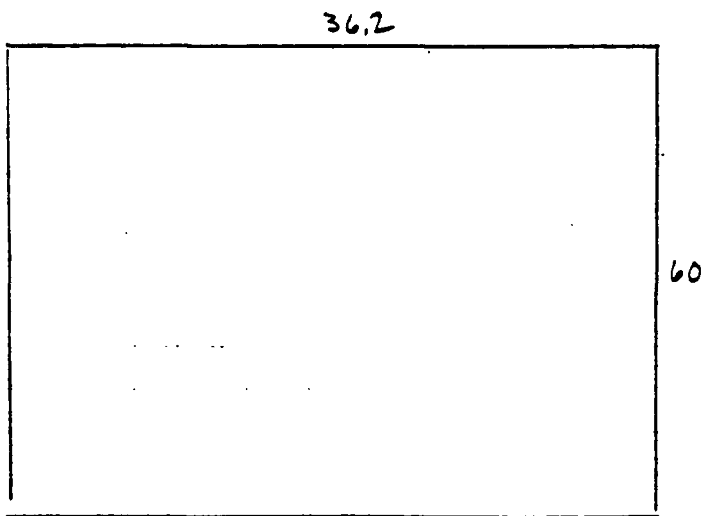

FIGURE 5-8

PROJECTED AREA OF INNER SHINGLE FOR HORIZONTAL (RADIAL) RESULTANT

$$F_x = 6.32(36.2)(60) = 13727 \text{ LB}$$

Total axial force = $6(2917 + 3862) = 40675\text{-}3$

For a S.F. = 1.4

$$F_z = 56945 \text{ LB}$$

5.5 SLEEC KINEMATIC RELATIONSHIPS

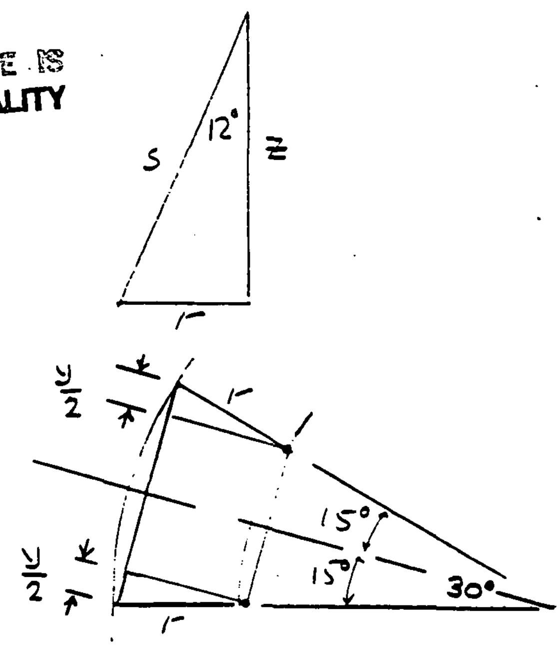

FIGURE 5-9

DEPLOYMENT GEOMETRY

s = displacement along shingle
z = axial displacement
r = radial displacement

$$s = \frac{z}{\cos 12°}$$

$$r = z \tan 12°$$

y = lateral growth

$$y = 2r \sin 15°$$

$$y = 2z \tan 12° \sin 15°$$

For $z = 60$ IN

$s = 61.34$ IN

$y = 6.602$ IN

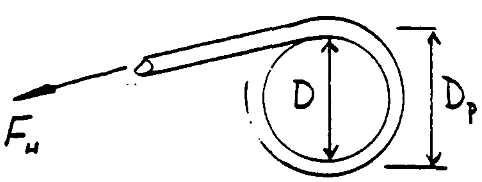

Cable Drum

Let Θ_B = ball screw rotation angle

$$\frac{\Theta_B}{2\pi} = \frac{s}{\Delta s}$$

where Δs = lead of the ball screw (length traveled in one revolution

$$\Theta_B = 2\pi \frac{s}{\Delta s}$$

$$\Theta_B = \frac{2\pi z}{\Delta s \cos 12°}$$

For $z = 60$ IN and $\Delta s = 1$ IN

$$\Theta_B = 2\pi (61.34)$$

Let Θ_s = cable drum rotation

$$y = \Theta_s \frac{D_p}{2}$$

$$\Theta_s = \frac{2y}{D_p} = \frac{4}{D_p} z \tan 12^\circ \sin 15^\circ$$

for $z = 60$

$D_p = 1.312$ in

$$\Theta_s = \frac{4(60)\tan 12 \sin 15}{1.312} = 10.063 \text{ rad}$$

$$\Theta_s = 1.602\ (2\pi) \text{ rad} \qquad (577^\circ)$$

The reduction ratio from the ball screw (spline, center drum) to the cable drum is the ratio of Θ_B to Θ_s

$$R = \frac{\Theta_B}{\Theta_s} = \frac{\dfrac{2\pi z}{\Delta s \cos 12^\circ}}{\dfrac{4 z \tan 12^\circ \sin 15^\circ}{D_p}}$$

$$R = \frac{\pi D_p}{2 \Delta s \sin 12^\circ \sin 15^\circ} = \frac{\pi (1.312)}{2(1) \sin 12^\circ \sin 15^\circ}$$

$$R = 38.30$$

5.6 SHINGLE LOADS ANALYSIS

Individual shingle pressure resultants have been determined

For the outer (larger) shingle the radial (x) outward component of resultant pressure and the axial (z) upward component of are respectively (including a 1.4 safety factor)

outer
$$F_x = 25{,}434 \text{ LB}$$
$$F_z = F_x \tan 12° = 5406 \text{ LB}$$

For the inner shingle these forces are

inner
$$F_x = 19{,}218 \text{ LB}$$
$$F_z = F_x \tan 12° = 4085 \text{ LB}$$

Figures 5-10 and 5-11 show projections of the freebodies of the two shingles in the xz and xy planes

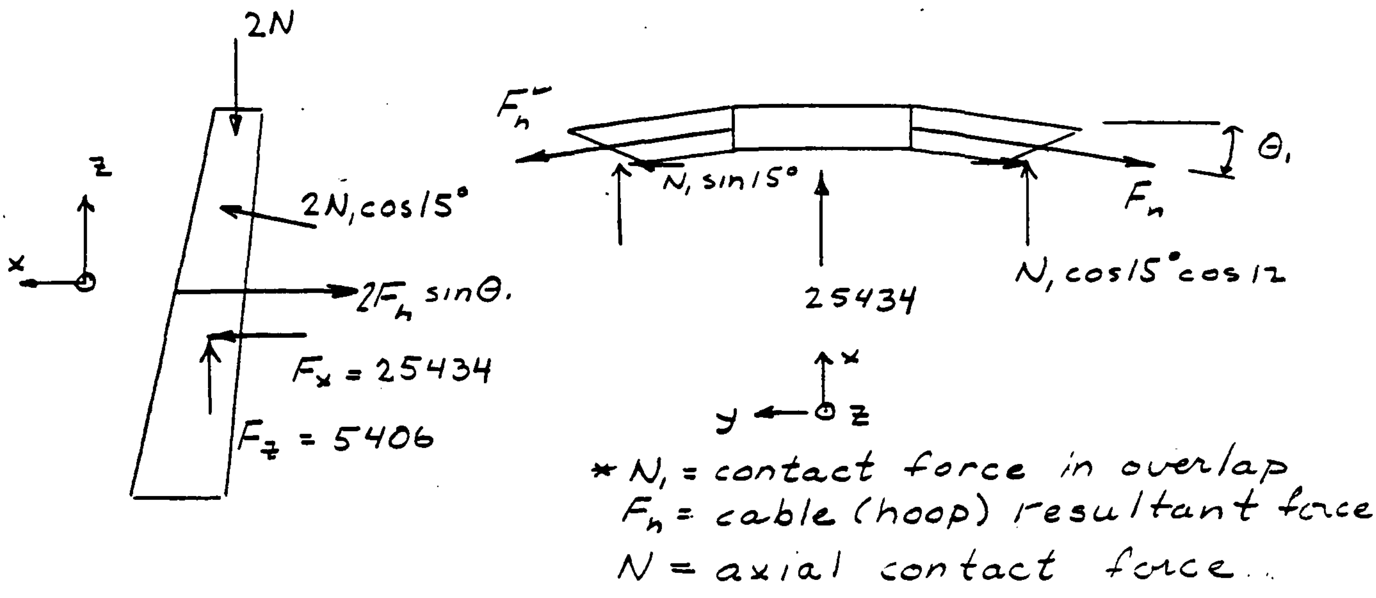

FIGURE 5-10

OUTER SHINGLE FREEBODY LOADS

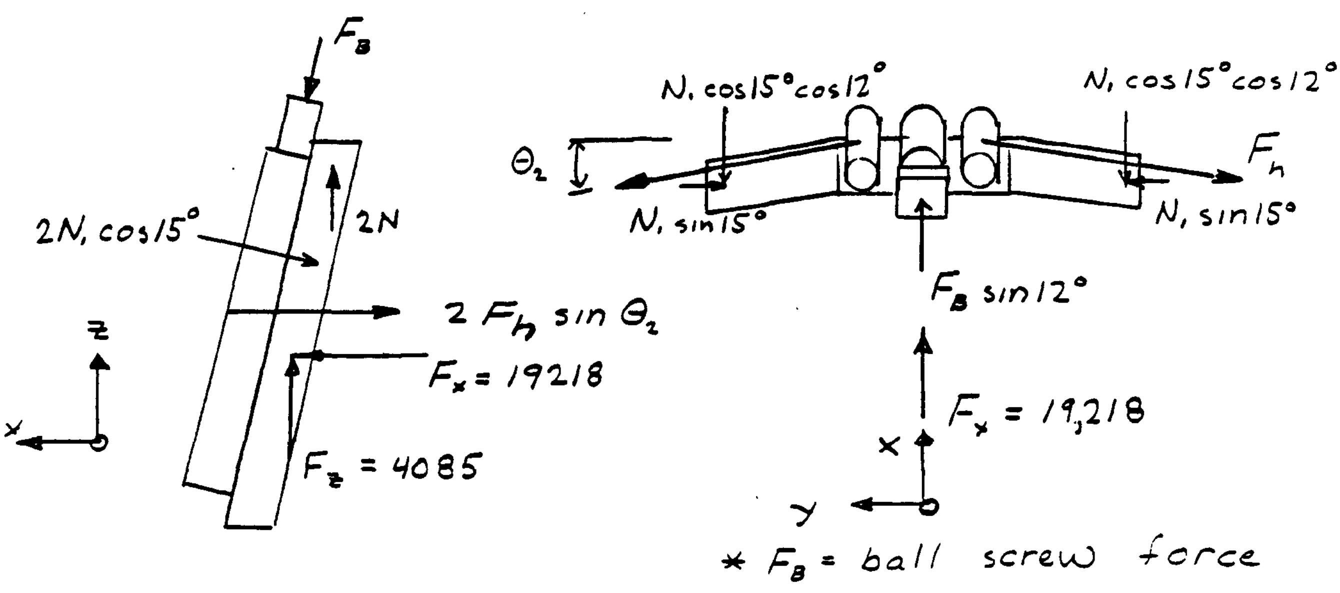

FIGURE 5-11

INNER SHINGLE FREEBODY LOADS

Write equilibrium equations for the two shingles.

Outer shingle

$\Sigma F_x = 0$

$$2F_h \sin\theta_1 = 25434 + 2N_1 \cos 15° \cos 12° \qquad (1)$$

$\Sigma F_z = 0$

$$2N = 5406 + 2N_1 \cos 15° \sin 12° \qquad (2)$$

Inner Shingle

$\Sigma F_x = 0$

$$2F_h \sin\theta_2 = 19218 - 2N_1 \cos 15° \cos 12° + F_B \sin 12° \qquad (3)$$

$\Sigma F_z = 0$

$$F_B \cos 12° = 2N + 4085 - 2N_1 \cos 15° \sin 12° \qquad (4)$$

Substitute equation (2) into equation (4)

$F_B \cos 12° = 5406 + 4085$

$F_B = 9703$ LB

Substitute this into equation 3

$$2F_h \sin\theta_2 = 21234 - 2N_1 \cos 15° \cos 12° \qquad (5)$$

Add equations (1) and (5)

$2F_h \sin\theta_1 + 2F_h \sin\theta_2 = 25{,}434 + 21{,}235$

$$2F_h \sin\theta_1 + 2F_h \sin\theta_2 = 46{,}669 \qquad (6)$$

The angles θ_1 and θ_2 are angles which the cables make with the normals to the centerlines of the respective shingles. Because the angle between the centerlines is 30° the sum of Θ_1 and Θ_2 is 30°.

Assume that the angles are equal

$$\Theta_1 = \Theta_2 = 15°$$

$$4F_h \sin 15° = 46669$$

$$F_h = 45{,}079 \text{ LB}$$

Subtract equations (1) and 5

$$2F_h \sin\Theta_1 - 2F_h \sin\Theta_2 = 4200 + 4N_1 \cos 15° \cos 12° \quad (7)$$

For $\Theta_1 = \Theta_2 = 15°$

$$0 = 4200 + 4N_1 \cos 15° \cos 12°$$

$$N_1 = -1111 \text{ LB}$$

The negative sign on N_1 indicates that a tensile rather than a compressive bearing force exists between the shingles. This of course is not possible. This condition occurs because the radial pressure resultant on the outer (larger) shingle at full extension is greater than the radial pressure resultant plus the radial component of ball screw thrust on the inner shingle.

Consider the case in which N_1 equals zero. Equations (7) and (5) give

$$2F_n(\sin\theta_1 - \sin\theta_2) = 4200 \text{ LB} \quad (8)$$

$$2F_n(\sin\theta_1 + \sin\theta_2) = 46669 \text{ LB} \quad (9)$$

Solve (9) for $2F_n$ and substitute in (8)

$$2F_n = \frac{46669}{\sin\theta_1 + \sin\theta_2}$$

The result is

$$\frac{\sin\theta_1 - \sin\theta_2}{\sin\theta_1 + \sin\theta_2} = \frac{4200}{46669} = .09000 \quad (10)$$

where

$$\theta_1 + \theta_2 = 30° \quad (11)$$

Solving equations (10) and (11) by trial and error

$$\theta_1 = 16.381°$$
$$\theta_2 = 13.618°$$

If θ_1 is increased beyond 16.381° (and θ_2 is decreased) the normal contact force becomes positive. This is necessary to provide a gas seal.

Assume

$\Theta_1 = 17^\circ$ (angle between cable and the normal to the outer shingle centerline)

$\Theta_2 = 13^\circ$ (angle between cable and the normal to the inner shingle centerline)

Solve equation (6)

$$2F_h(\sin 17^\circ + \sin 13^\circ) = 46{,}669$$

$$F_h = 45{,}106 \text{ LB}$$

Substitute in equation (1) to find N_1

$$2N_1 \cos 15^\circ \cos 12^\circ = 2(45106)\sin 17^\circ - 25434$$

$$N_1 = 498 \text{ LB}$$

Design forces assuming Θ_1 is 17° and Θ_2 is 13° are then

F_B (ball screw thrust) = 9702 LB

F_H (hoop tension resultant) = 45106 LB

N_1 (overlap bearing force) = 498 LB

5.7 Component Loads Analysis

5.7.1. Ball Screw Loads

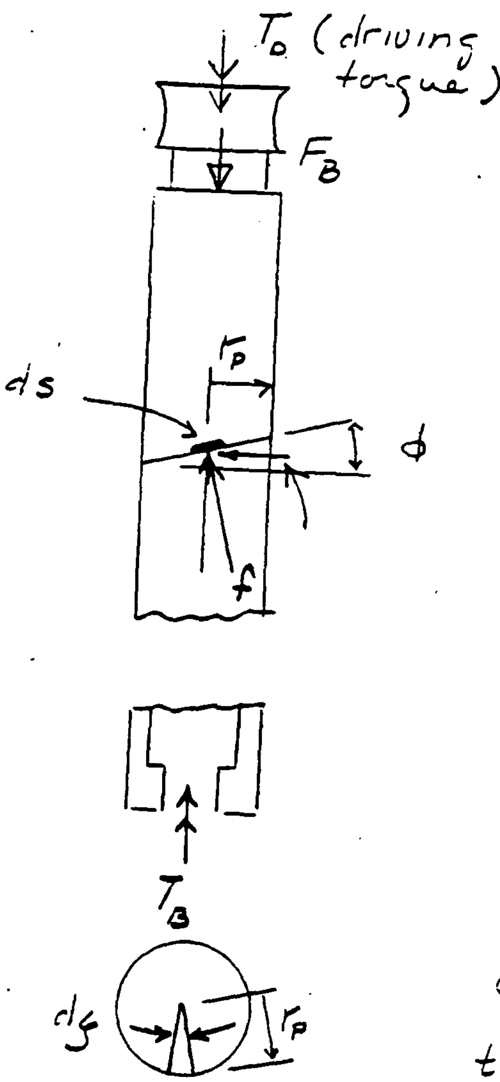

Let f be the force per unit length of thread between the ball screw and nut. The angle ϕ is the screw lead angle, r_p is the pitch radius and N is the number of turns in the nut

The axial force acting on the infinitesimal thread length ds is (assuming no friction)

$$dF_B = f\,ds\,\cos\phi$$

$$ds = \frac{r_p\,d\xi}{\cos\phi}$$

$$dF_B = f\,r_p\,d\xi$$

Integrating over the length of the screw gives

$$F_B = f\,r_p\,2\pi N \qquad (1)$$

The tangential component of the ball screw force on elemental length ds is

$$dF_t = f\,ds\,\sin\phi = f\frac{r_p\,d\varsigma}{\cos\phi}\sin\phi$$

$$dF_t = f\,r_p\tan\phi\,d\varsigma$$

Torque due to this tangential component is

$$dT_B = dF_t\,r_p = f\,r_p^2\tan\phi\,d\varsigma$$

Integrating gives the torque in the ball screw nut

$$T_B = f\,r_p^2\tan\phi\;2\pi N \qquad (2)$$

From equation (1)

$$f = \frac{F_B}{2\pi N r_p} \qquad (3)$$

Substitute (3) into (2)

$$T_B = \frac{F_B}{2\pi N r_p}\,r_p^2\tan\phi\;2\pi N$$

$$T_B = F_B\,r_p\tan\phi \qquad (4)$$

Let Δs be the lead on the ball screw (the screw advances Δs for each revolution of the screw)

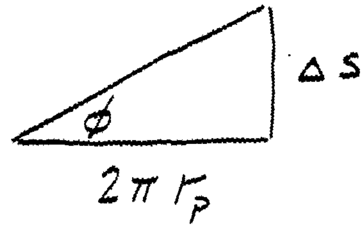

The lead and lead angle are related by the equation

$$\tan \phi = \frac{\Delta S}{2\pi r_p} \qquad (5)$$

Substituting (5) into (4) gives

$$T_B = F_B r_p \frac{\Delta S}{2\pi r_p}$$

$$T_B = F_B \frac{\Delta S}{2\pi}$$

For

$$F_B = 9702 \text{ LB}$$

$$\Delta S = 1 \text{ IN}$$

$$T_B = \frac{9702}{2\pi} = 1544 \text{ IN-LB}$$

A free body of the ball screw is shown below

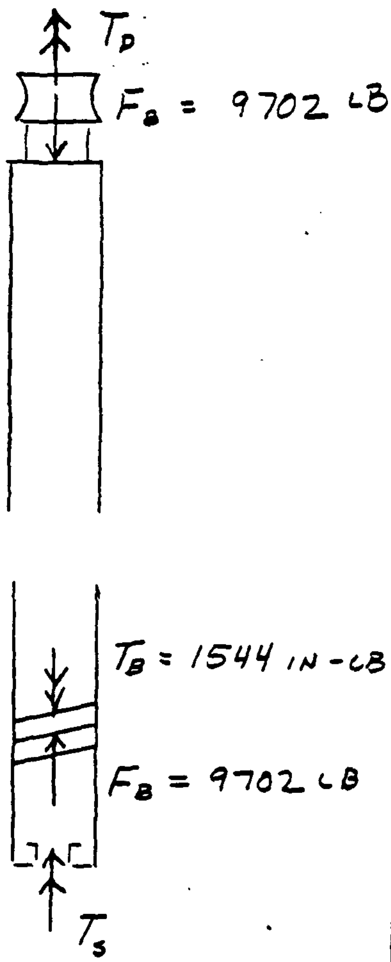

FIGURE 5-12

BALLSCREW FREEBODY LOADS

The driving torque from flex cable (through the gear box) is T_D where

$$T_D + T_S = T_B$$

In considering the freebodies of the system components it will be shown that

$$T_S = T_B$$

so that $T_D = 0$ and no driving torque is necessary as long as the kinematic relations allow the cone to extend along the constant cone angle

Free bodies of the splined shaft, the housing the reduction gear box from the housing to the roller housing and the roller are shown in figure 5-13

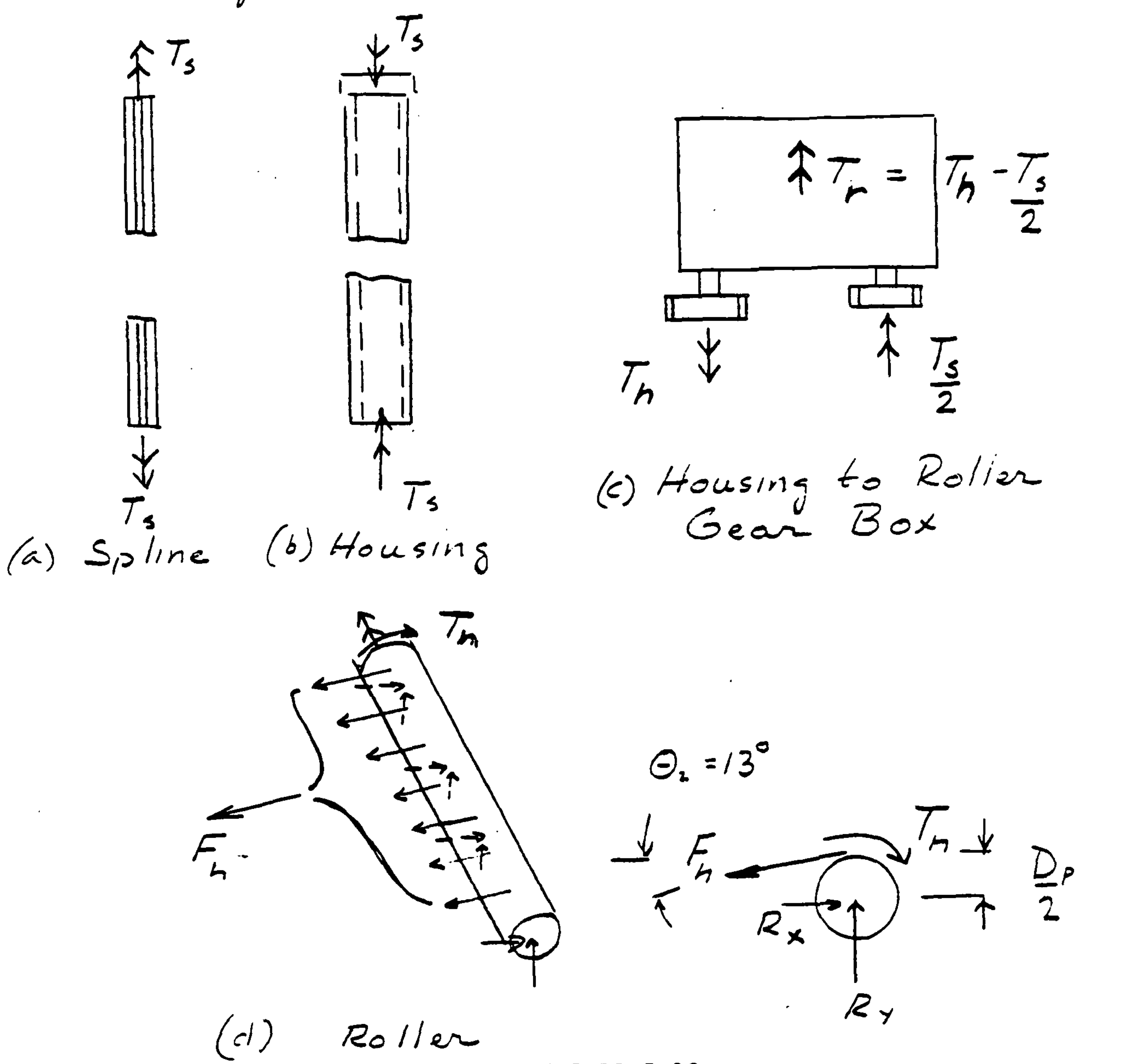

FIGURE 5-13

COMPONENT FREEBODIES LOADS

Considering the roller free body

$$\Sigma M_z = 0$$

$$T_h = F_h \frac{D_p}{2}$$

where

$$F_h = 45{,}106 \text{ LB}$$

$$D_p = 1.312 \text{ IN}$$

$$T_h = 45{,}106 \left(\frac{1.312}{2}\right) = 29{,}590 \text{ IN-LB}$$

The torque T_s into the housing-roller gear box is related to T_h by the expression

$$T_s = \frac{T_h}{R}$$

where from kinematics of the system

$$R = \frac{\pi D_p}{2 \Delta s \sin 12^\circ \sin 15^\circ} = 38.30$$

Spline torque T_s is then

$$\frac{T_s}{2} = \frac{29590}{38.30}$$

$$T_s = 1545 \text{ IN-LB}$$

Note that this torque is the same as the ball screw torque (1545 IN-LB to 1544 IN-LB) proving that the driving torque is zero for no friction. The reaction torque from the housing - roller gear box is

$$T_r = T_h - \frac{T_s}{2}$$

$$T_r = 28{,}888 \text{ IN-LB}$$

This torque acts on the gear box - ball screw flange and is internally balanced by the opposite side roller housing gear box. Figure 5-14 shows a freebody of the mounting flange

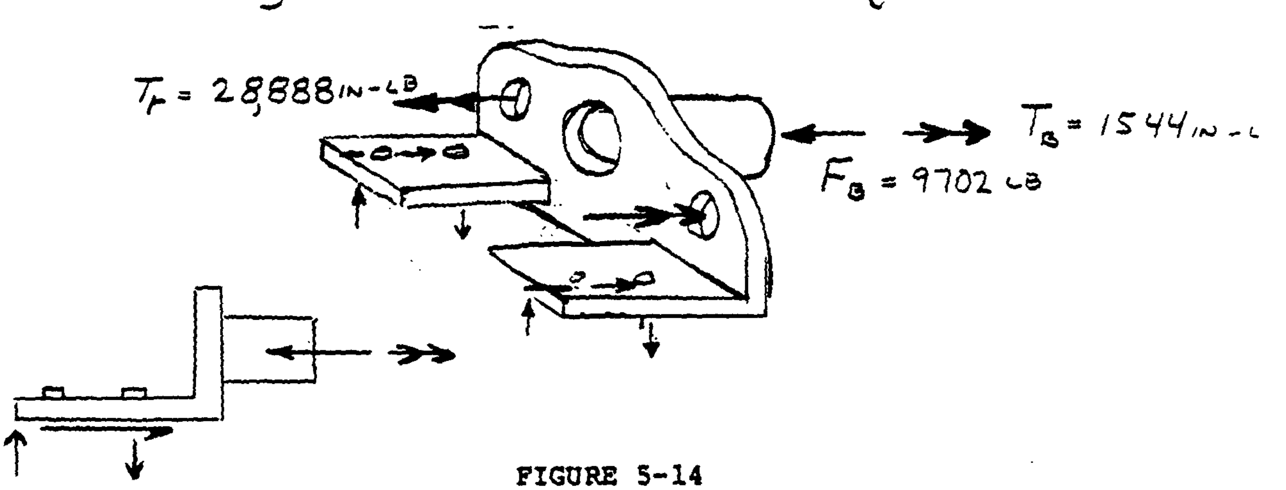

FIGURE 5-14

MOUNTING BRACKET FREEBODY LOADS

From Figure 5-13(d) the total reactions between the roller and the six bracket are

$$R_y = F_n \cos 13^\circ = 45106 \cos 13 = 43950 \text{ LB}$$

$$R_y = F_n \sin 13^\circ = 45106 \sin 13 = 10{,}147 \text{ LB}$$

Assume that the reactions vary linearly from the top bracket to the bottom

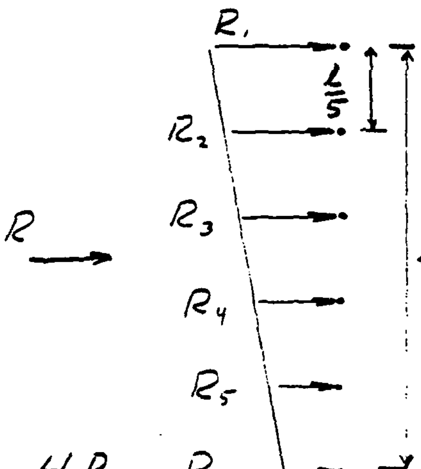

$.4 R_1 = R_6$

Assume that the bottom reaction is .4 times the top reaction (approximately the ratio of the products of pressure times diameter at the top and bottom)

$$\Delta R = \frac{.6 R_1}{l} \frac{l}{5}$$

$$R_2 = R_1 - \frac{.6R_1}{l}\left(\frac{l}{5}\right) = .88R_1$$

$$R_3 = R_1 - \frac{.6R_1}{l}\left(\frac{2l}{5}\right) = .76R_1$$

$$R_4 = R_1 - \frac{.6R_1}{l}\left(\frac{3l}{5}\right) = .64R_1$$

$$R_5 = R_1 - \frac{.6R_1}{l}\left(\frac{4l}{5}\right) = .52R_1$$

$$R_6 = .4R_1$$

$$R_1(.88+.76+.64+.52+.4) = R$$

$$3.2\,R_1 = R$$

$$3.2\,R_{x_1} = 43{,}950$$

$$R_{x_1} = 13734\text{ LB}$$

$$3.2\,R_{y_1} = 10147$$

$$R_{y_1} = 3171\text{ LB}$$

The top bracket is shown in figure 6

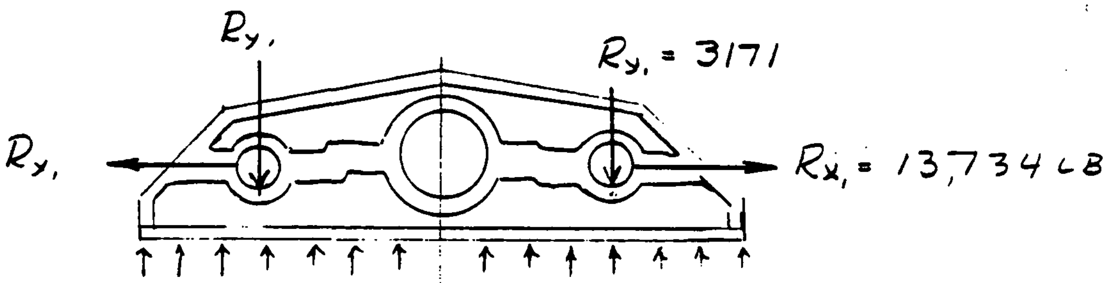

FIGURE 5-15

TOP BRACKET FREEBODY LOADS

5.8 COMPONENT STRESS ANALYSIS

5.8.1. Ball Screw – Buckling

Assume the ends of the ball screw are free to rotate (worst case)

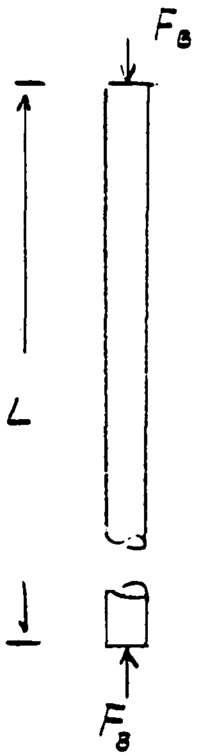

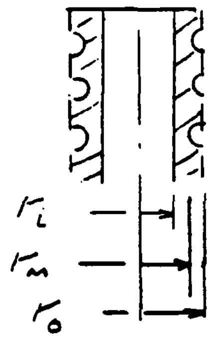

Critical buckling load is given by

$$F_{crit} = \frac{\pi^2 E I}{L^2}$$

$E = 29 \times 10^6$

$L = 63$ IN

$$I = \frac{\pi}{4}(r_e^4 - r_i^4)$$

where r_e is the effective outside radius.

$r_M < r_e < r_o$

For a conservative result let

$r_e = r_M = .78$ IN

$r_i = .56$ IN

$$F_{crit} = \frac{\pi^2 (29 \times 10^6)}{(63)^2} \frac{\pi}{4} (.78^4 - .56^4)$$

$F_{crit} = 15394$ LB

$$M.S. = \frac{F_{CRIT}}{F_B} - 1 = \frac{15394}{9702} - 1 = 0.\underline{\underline{587}}$$

5.8.2. Spline Shear Stress

$$\tau = \frac{2T}{\pi r^3}$$

$$r = .42''$$

$$\tau = \frac{2(1545)}{\pi(.42)^3} = 13276 \text{ psi}$$

5.8.3. Housing Shear stress

$$\tau = \frac{2T r_o}{\pi(r_o^4 - r_i^4)}$$

$$r_o = 1.1$$

$$r_i = 0.92$$

$$\tau = \frac{2(1545)(1.1)}{\pi(1.1^4 - .92^4)} = 1447 \text{ psi}$$

5.8.4. Cable Drum Shear Stress

$$\tau = \frac{16 M_t}{\pi d^3}$$

$$M_t = 29590 \text{ in-lb}$$

$$d = 1.125$$

$$\tau = \frac{16(29590)}{\pi(1.125)^3} = 105{,}842 \text{ psi}$$

Use AISI S7 tool steel tempered at 800°F. Material properties are

$$F_{Tu} = 275$$

$$F_{Ty} = 205$$

$$e = 10\% \text{ (in 2 in gage length)}$$

Assume that the shear yield is .6 times the tensile yield stress

$$F_{Sy} = 123 \text{ ksi}$$

$$M.S._L = \frac{F_{sy}}{\tau} - 1 = \frac{123}{105.842} - 1$$

$$M.S._L = \underline{\underline{0.162}}$$

5.B.5. Cable Tension

Assume the cable tension varies linearly from F_1 at the top to $.4F_1$ at the bottom of the shingle. This is approximately the ratio of pR at the top and bottom of the nozzle, where p is pressure and R is cone radius.

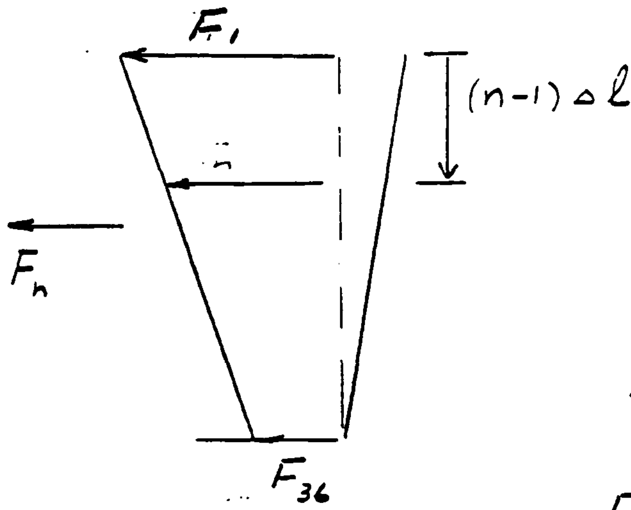

$$F_{36} = .4\,F_1$$

$$\Delta F = \frac{F_1 - F_{36}}{35} = \frac{.6\,F_1}{35}$$

$$F_n = F_1 - (n-1)\frac{.6\,F_1}{35}$$

$$F_n = F_1\left[1 - (n-1)\frac{.6}{35}\right]$$

$$1 \le n \le 36$$

$$\sum F_n = F_h$$

$$F_1\left\{1 + \left[1 - \frac{.6}{35}\right] + \left[1 - \frac{2(.6)}{35}\right] + \left[1 - \frac{3(.6)}{35}\right] - - - + \left[1 - \frac{35}{35}(.6)\right]\right\} = F_h$$

$$F_1\left\{36 - \frac{.6}{35}\left[1 + 2 + 3 + \cdots + 35\right]\right\} = F_h$$

$$F_1\left\{36 - \frac{.6}{35}(630)\right\} = F_h$$

$$F_1 = \frac{F_h}{25.2}$$

$$F_1 = \frac{45106}{25.2} = 1790\ \text{LB}$$

The 3/16 inch cable will support 3700LB (ref Table 1 MIL-W-83420D)

$$M.S. = \frac{F_{allow}}{F_1} - 1 = \frac{3700}{1790} - 1 = \underline{\underline{1.07}}$$

5.8.6. Cable Retension Force

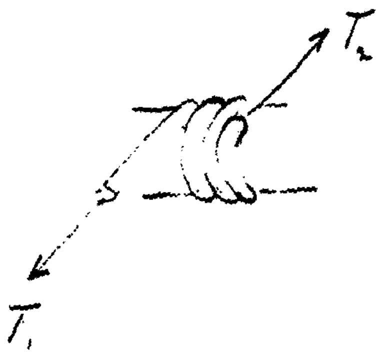

$$T_2 = \frac{T_1}{e^{\mu\theta}}$$

μ = friction factor
θ = wrap angle

$T_{1\,max} = 1790$

For $\mu = .25$

For $\theta = 2\pi$ (1 wrap)

$$T_2 = \frac{1790}{e^{(.25)(2\pi)}} = 372 \text{ LB}$$

For $\theta = 2(2\pi)$ (2 wraps)

$$T_2 = \frac{1790}{e^{(.25)4\pi}} = 77 \text{ LB}$$

The current design uses one full wrap of cable still in contact with the roller at full extension. For this case the cable connection need only develope a 372 LB force to balance the maximum cable force of 1790 LB

5.8.7. Cable Drum Bending Stress

The cables induce bending as well as twisting moments into the cable drum

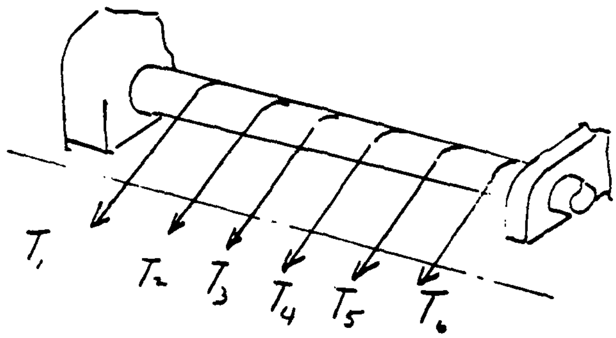

$T_1 = 1790$

$T_2 = 1759$

$T_3 = 1729$

$T_4 = 1698$

$T_5 = 1667$

$T_6 = 1637$

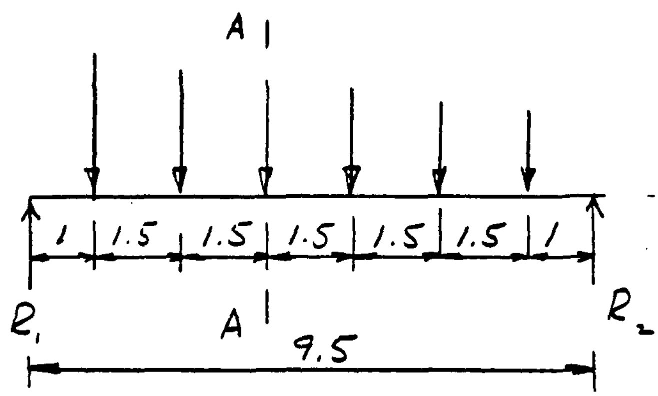

Assume simple supports (conservative)

$$9.5R_1 = 1790(8.5) + 1759(7) + 1729(5.5) + 1698(4) + 1667(2.5) + 1637(1)$$

$$R_1 = 5225 \text{ LB}$$

Maximum bending moment occurs at section AA.

$$M_{AA} = 5225(4) - 1790(3) - 1759(1.5)$$

$$M_{AA} = 12892 \text{ IN-LB}$$

Maximum bending stress is

$$\sigma_B = \frac{Mc}{I} = \frac{32M}{\pi d^3}$$

where $d = 1.125$ in

$$\sigma_B = \frac{32(12892)}{\pi\,(1.125)^3} = 92,224 \text{ psi}$$

For AISI H7 tool steel

$$F_{Ty} = 205^{\text{ksi}}$$

$$M.S. = \frac{F_{Ty}}{\sigma_B} - 1 = \frac{205}{92.224} - 1 = \underline{\underline{1.223}}$$

5.8.8 Combined Stress Due to Torsion and Bending

At section AA in addition to bending moment a torsional moment exists

$$M_{t_{AA}} = 29590 - (1790 + 1759 + 1729)(1.312)$$

$$M_{t_{AA}} = 22665 \text{ IN-LB}$$

$$\tau_{AA} = \frac{16 M_{t_{AA}}}{\pi d^3} = \frac{16(22665)}{\pi(1.125)^3} = 81072 \text{ psi}$$

$$\sigma_{B_{AA}} = 92,224 \text{ psi}$$

Maximum shear stress (refer to Mohr's circle) is given by

$$\tau_{max} = \left[\left(\frac{\sigma_B}{2}\right)^2 + \tau^2 \right]^{\frac{1}{2}}$$

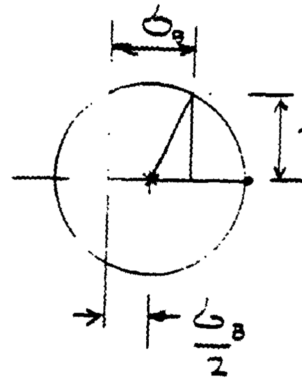

$$\tau_{max} = \left[\left(\frac{92224}{2}\right)^2 + (81072)^2 \right]^{\frac{1}{2}}$$

$$\tau_{max} = 93{,}267 \text{ psi}$$

This is less than max shear stress at the gear head and is not critical

$$M.S = \frac{123000}{93267} - 1 = 0.319$$

5.8.9 Main Mounting Flange Bending Stress

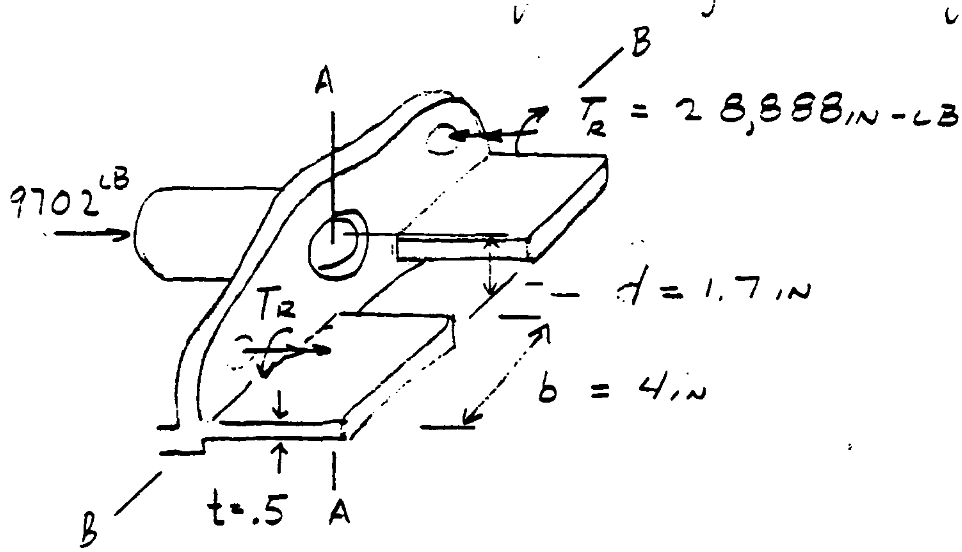

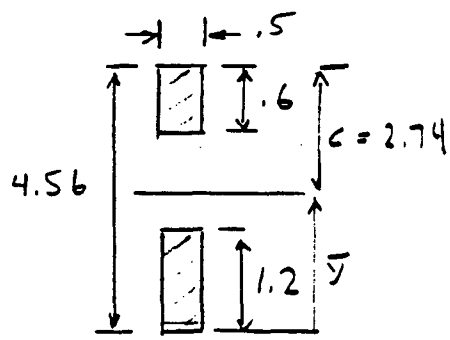

AA

A	$\bar{y}$	$A\bar{y}$	d	Ad^2	I
.5(.6) = .30	4.26	1.278	2.44	1.786	.009
.5(1.2) = .60	.6	.36	1.32	1.045	.072
.90		1.638			

$$\bar{y} = \frac{1.638}{.90} = 1.82$$

$$I_{AA} = 2.912$$

Bending stress at section AA due to the torque T_R is

$$\sigma_{AA} = \frac{T_R\, c}{I} = \frac{28{,}888\,(2.74)}{2.912}$$

$$\sigma_{AA} = 27{,}182$$

$$F_{Ty} = 90^{KSI}$$

$$M.S. = \frac{90}{27.182} - 1 = 2.3$$

Bending stress at BB due to the eccentric ball screw thrust force is

$$\sigma_{BB} = \frac{6 F_b d}{2 b t^2} = \frac{6(9702)(1.7)}{2(4)(.5)^2} = 49{,}480 \text{psi}$$

Material is a 17-4ph casting
Use two-thirds of the MIL-HDBK 5D value for tensile yield

$$F_{T_y} = 90^{ksi}$$

$$M.S. = \frac{F_{T_y}}{\sigma_{BB}} - 1 = \frac{90}{49.48} - 1 = \underline{\underline{0.819}}$$

5.9 SLEEC Response to Side Load

As it is currently configured the SLEEC support structure (six ball screws essentially pinned at each end) offers little resistance to side load. Any appreciable side load will move the extendible cone against the fixed cone which then reacts load in bearing

In the ground check mode the SLEEC will be deployed with the SRB in the horizontal position. This constitutes deployment with a 1 g side load and no internal pressure Figure 5-16 shows a freebody of the cone in the fully extended position.

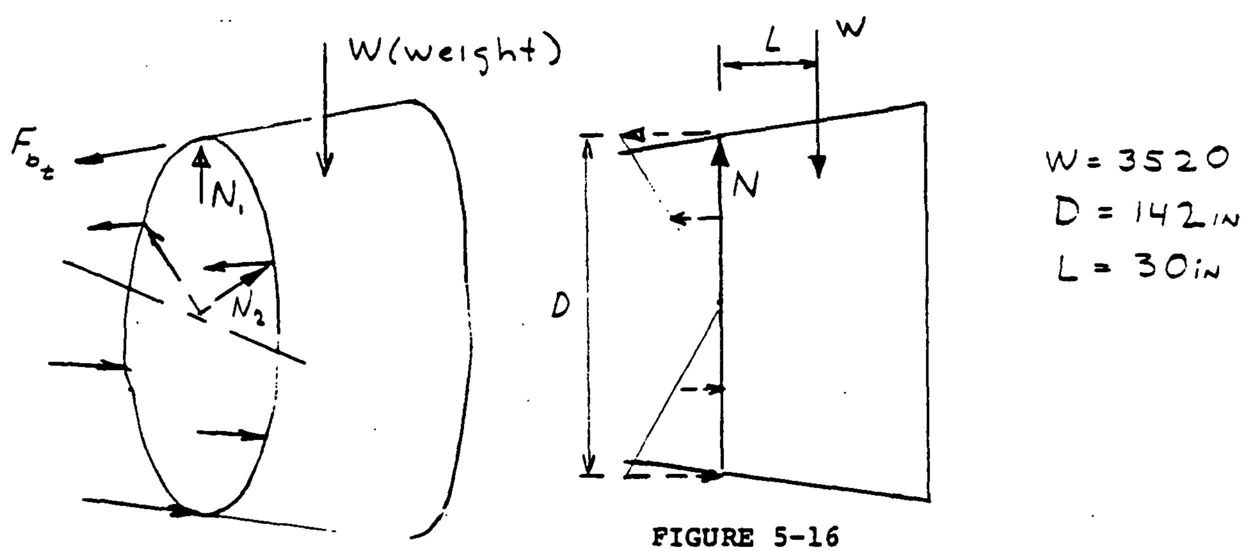

FIGURE 5-16

SLEEC WITH 1-G SIDE LOAD

Assume the ball screw forces are axial and that their horizontal components vary linearly from the cone mid-plane

$$\Sigma M_o = 0$$

$$F_1 D + F_1 \sin 30° D \sin 30° = WL$$

$$F_1 = \frac{WL}{1.5D} = \frac{3530(30)}{1.5(142)} = 497 \text{ LB}$$

The axial force in the top ball screw is

$$F_{B_t} = \frac{497}{\cos 12°} = 508 \text{ LB}$$

The bottom ball screw has an equal compression. The vertical component of the ball screw forces is

$$F_v = 2(508)\sin 12° + 4(254)\sin 12 \sin 30°$$

$$F_v = 318 \text{ LB}$$

Summing vertical forces the resultant contact force with the fixed cone is

$$N = 3848 \text{ LB}$$

Assuming the to shingle carries a normal force N_1 and the two side shingles a normal force of $N_1 \sin 30°$

$$N_1 + 2 N_1 \sin^2 30° = 3848$$

$$N_1 = 2564 \text{ LB}$$

$$N_2 = 2565 \sin 30° = 1282 \text{ LB}$$

ORIGINAL PAGE IS
OF POOR QUALITY

Consider a free body of the upper half of the SLEEC

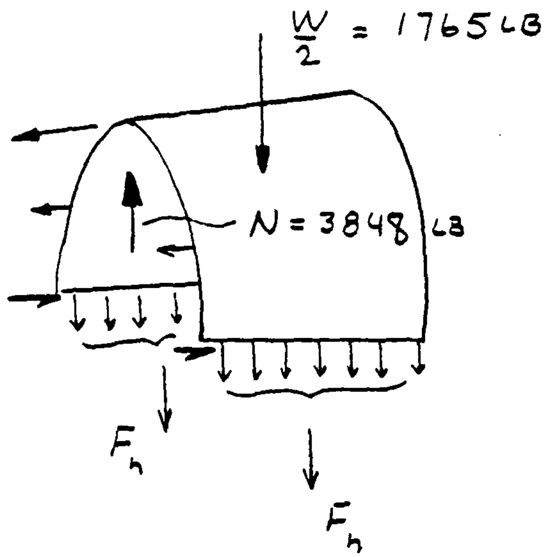

The cable resultant at mid-plane is F_h

Summing vertical forces

$$2F_h = 3848 - 1765 - 159$$

$$F_h = 963 \text{ LB}$$

The mid-plane cables are therefore in tension. Similar free bodies for other circumferential segments show that the cables always appear to be in tension. It may prove that the removable compression struts which have been proposed for the ground check mode are not necessary.

Mechanical Components

SECTION 6

MECHANICAL COMPONENTS

6.1 GEARS

Figure 6-1 schematically illustrates the transfer of power from the flexshaft to the parallel cable drums through the worm gear set, spur gear train, and internal differential reduction gear system.

The internal differential consists of a compound sun gear, six component planet gears, a fixed ring, and a rotating ring which is coupled by means of a spline to the respective cable drums. The gear ratio for the system is 37.5:1. Planetary gearing was selected because of the inherent advantages it offers in overall envelope and gear tooth load reduction.

The spur gears of the SLEEC actuation system have been designed to AGMA standards. Gear pitch diameters, diametral pitches, and facewidths have been selected to provide a balanced design for gear tooth strength.

The material selected for all spur gears is AMS6265 (AISI 9310 vacuum melt) steel. The gears will be case-carburized to Rockwell C60 minimum hardness, with a mimimum core hardness of Rockwell C33. All gears will be ground to AGMA quality grade 10+. Ground surfaces will have a 32 RMS finish.

6.1.1 Spur Gear Tooth Stresses

Gear stresses were calculated in accordance with the AGMA Standard 218.01 for pitting resistance and bending strength and AGMA Standard 226.01 for geometric factors. In addition, gear tooth face widths and diametral pitches were chosen so that the derating factors for bending and compressive stress are greater than one. The following paragraphs present the stress and derating factor equations.

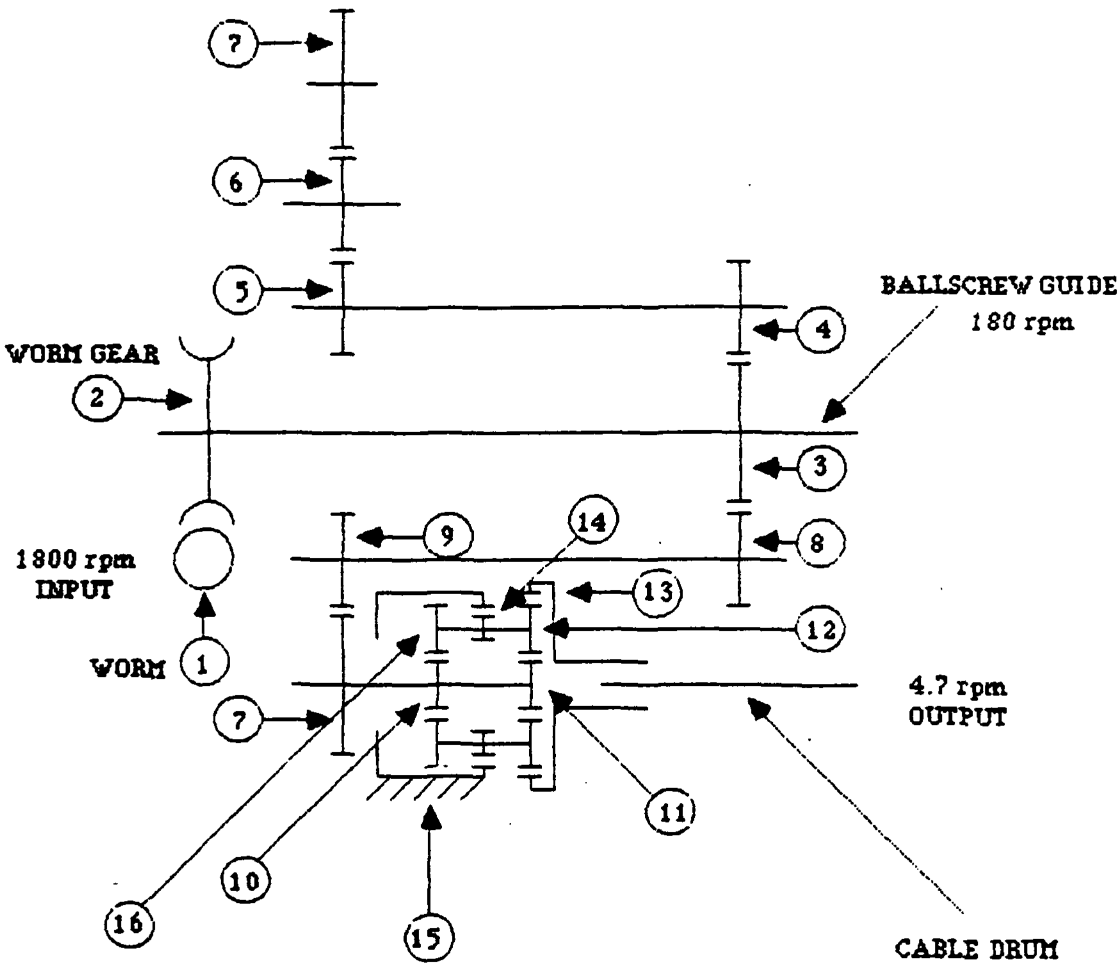

FIGURE 6-1

GEAR SCHEMATIC (BALLSCREW AND CABLE DRUM)
SLEEC ACTUATION SYSTEM

6.1.2 Compressive Stress

Compressive stress was calculated from the formula:

$$S_c = C_p \left[\left(\frac{W_t \, C_o}{C_v} \right) \left(\frac{C_s}{dF} \right) \left(\frac{C_m C_f}{I} \right) \right]^{1/2}$$

where

- S_c = maximum compressive stress, psi
- C_p = elastic coefficient (2290 for steel at room temperature)
- W_t = tangential tooth load, lb
- C_o = overload factor (1.0 for uniform loading)
- C_v = dynamic factor (1.0 for gears ground to high accuracy)
- F = minimum face width, in
- d = pinion pitch diameter, in
- C_s = size factor (1.0 for hardened and ground gears)
- C_m = load distribution factor (1.0 for rigidly-mounted, accurately ground gears)
- C_f = surface condition factor (1.0 for high-quality ground surface finish)
- I = geometric factor (calculated by digital computer from the formulas in Appendix A of the AGMA Standard 218.01)

The derating factor for tooth wear was calculated from the formula:

$$DF_C = \frac{S_{CANC}}{S_c}$$

where:

- DF_C = compressive stress derating factor

S_{CANC} = allowable compressive stress at the number of tooth contact cycles required, psi

S_c = calculated compressive stress, psi

6.1.3 Bending Stress

Bending stress was calculated from the formula:

$$S_t = \left(\frac{W_t K_o}{K_v}\right)\left(\frac{P_d}{F}\right)\left(\frac{K_s K_m}{J}\right)$$

where:

S_t = calculated tensile stress at the root of the tooth, psi

W_t = tangential tooth load, lb

K_o = overload factor (1.0 for uniform loading)

K_v = dynamic factor (1.0 for gears ground to high accuracy)

P_d = diametral pitch at the large end of the gear tooth

F = minimum face width, in

K_s = size factor (1.0 for hardened and ground gears)

K_m = load distribution factor (1.0 for rigidly-mounted, accurately ground gears)

J = geometric factor (calculated by digital computer from the formulas in Appendix B of AGMA Standard 218.01)

The derating factor for tooth strength was calculated from the formula:

$$DF_B = \frac{S_{BANC}\ K_i}{S_t}$$

where:

DF_B = bending stress derating factor

S_{BANC} = allowable tensile bending stress at the number of tooth contact cycles required

K_i = load reversal factor (0.75 for gears subjected to revese bending, otherwise use K_i = 1.0)

S_t = calculated root tensile stress, psi

Table 6-1 is a summary of the SLEEC gear design.

6.2 BEARINGS

The proposed SLEEC actuation system utilizes rolling-element bearings on the ballscrew shafts, cable drums, and geartrains. Bearing locations are shown in Figures 6-2 and 6-3.

The ballscrew and cable drum shafts incorporate needle roller bearings utilizing the high load-carrying capacity of a roller bearing for the limited space available.

The spur gears are supported by radial ball bearings that provide a rigid and well-aligned mounting for the gears.

The bearing selection summary is presented in Table 6-2.

TABLE 6-1

GEAR DESIGN
SLEEC ACTUATION SYSTEM

No.	No. of Teeth	Diametral Pitch	Operating Pressure Angle	Face Width	Design Point: Speed	Torque	Tooth Load,	Bending Stress	Compressive Stres	Calculated Life
			deg	in	rpm	in-lbs	lb	psi	psi	hrs
1	2	10	14.5	.833	1800	102	813	9889(2)	----	----
2	20	"	"	"	180	771	"	" (2)	----	----
3	90	32	25	.45	"	1514	537	92774	192437	90.3
4	48	"	"	.50	338	402	"	90949	"	180
5	47	"	"	"	"	"	547	91747	211921	136
6	"	"	"	"	"	"	"	90594	195477	4.29
7	90	"	"	.45	176	771	"	94266	"	109
8	48	"	"	.50	338	402	537	90949	192437	180
9	47	"	"	"	"	"	547	90594	195477	4.29
10	24	17	"	.70	176	386	88	5730	73982	>1000
11	"	"	"	"	"	"	"	"	"	"
12	18	"	"	.75	172	1446	2660	131885	255372	2.02
13	60	"	"	.70	4.7	28913	"	102902	"	39.3
14	18	19	"	.75	172	1349	2837	141210	296742	1.06
15	66	"	"	.70	0	29678	"	135689	"	2.34
16	18	17	"	.75	172	48	88	5348	73982	>1000

NOTES:
(1) Spur gear design based on 99%
(2) Unit load for worm gear set
(3) All spur gears are manufactured from vacuum melt 9310 (AMS-6265) and cerburized
(4) Design Lige-One Deployment (20 sec)

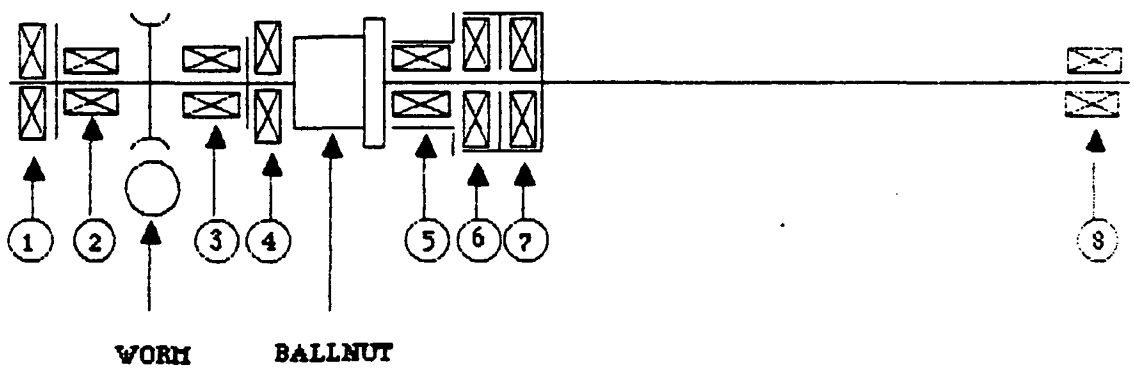

FIGURE 6-2

BEARING SCHEMATIC FOR THE SLEEC
ACTUATION SYSTEM BALLSCREWS

ORIGINAL PAGE IS
OF POOR QUALITY

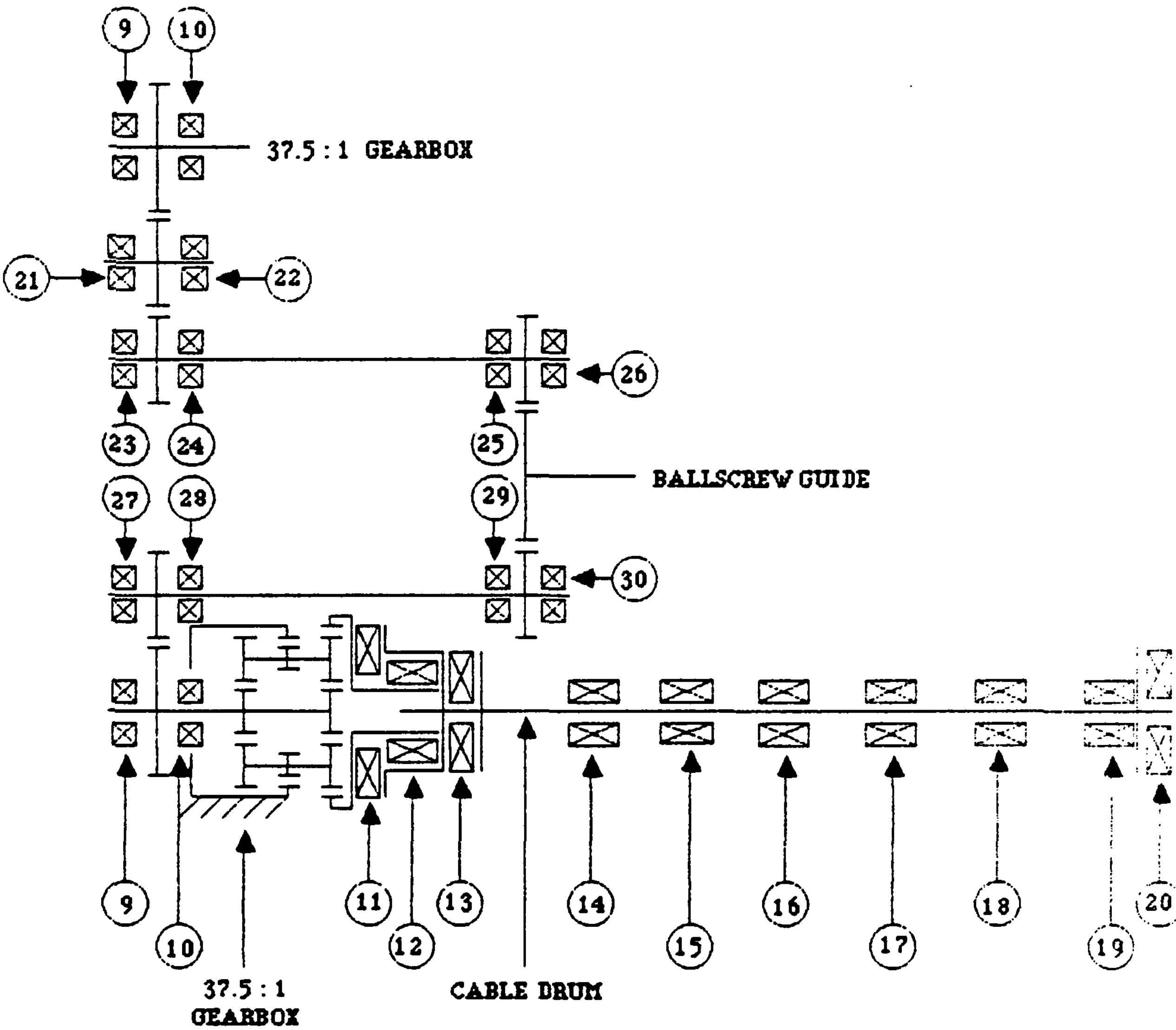

FIGURE 6-3

BEARING SCHEMATIC FOR THE SLEEC
ACTAUTION SYSTEM CABLE DRUM

TABLE 6-2

BEARING SUMMARY SLEEC ACTUATION SYSTEM

No.	Position	Size	Type	Material	Part No.	Bore-O.D.-Width	Separator	Static Capacity	Dynamic Capacity	Speed	B_1 Life
						in		lb	lb	rpm	hrs
1	Ballscrew	--	Needle	52100	--	1.0-1.562-0.0781	2-Piece	4360	2410	180	8400 (1)
2	Ballscrew	--	Needle	52100	--	0.75-1.0-0.500	None	2630	2700	180	8400 (1)
3	Ballscrew	--	Needle	52100	--	1.0-1.25-0.50	None	3410	3170	180	1890 (1)
4	Ballscrew	--	Needle	52100	--	1.502-2.97-0.25	2-Piece	26100	15900	180	96 (1)
5	Ballscrew	--	Needle	52100	--	2.25-2.625-0.75	None	12000	8860	180	357 (1)
6	Ballscrew	--	Needle	52100	--	2.5-3.25-0.0781	2-Piece	13100	4650	180	8400 (1)
7	Ballscrew	--	Needle	52100	--	2.5-3.25-0.0781	2-Piece	13100	4650	180	8400 (1)
8	Ballscrew	--	Needle	52100	--	2.25-2.625-0.75	None	12000	8860	180	8400 (1)
9	Gearset	104	Ball	52100	--	0.7874-1.6535-0.4724	2-Piece	1000	1620	176	7808
10	Gearset	104	Ball	52100	--	0.7874-1.6535-0.4724	2-Piece	1000	1620	176	7808
11	Cable Drum	--	Needle	52100	--	2.5-3.25-0.0781	2-Piece	13100	4650	4.7	1995 (1)
12	Cable Drum	--	Needle	52100	--	1.625-2.25-0.75	None	10100	7990	4.7	861 (1)
13	Cable Drum	--	Needle	52100	--	1.375-2.062-0.0781	2-Piece	8890	3820	4.7	1995 (1)
14	Cable Drum	--	Needle	52100	--	1.3125-1.625-0.625	None	5590	4900	4.7	21 (1)
15	Cable Drum	--	Needle	52100	--	1.3125-1.625-0.625	None	5590	4900	4.7	31 (1)
16	Cable Drum	--	Needle	52100	--	1.3125-1.625-0.625	None	5590	4900	4.7	50 (1)
17	Cable Drum	--	Needle	52100	--	1.3125-1.625-0.625	None	5590	4900	4.7	84 (1)
18	Cable Drum	--	Needle	52100	--	1.3125-1.625-0.625	None	5590	4900	4.7	157 (1)
19	Cable Drum	--	Needle	52100	--	1.3125-1.625-0.625	None	5590	4900	4.7	2310 (1)
20	Cable Drum	--	Needle	52100	--	0.50-0.937-0.0781	2-Piece	1520	1230	4.7	8400 (1)
21	Gearset	104	Ball	52100	--	0.7874-1.6535-0.4724	2-Piece	1000	1620	338	4089
22	Gearset	104	Ball	52100	--	0.7874-1.6535-0.4724	2-Piece	1000	1620	338	4089
23	Gearset	104	Ball	52100	--	0.7874-1.6535-0.4724	2-Piece	1000	1620	338	4089
24	Gearset	104	Ball	52100	--	0.7874-1.6535-0.4724	2-Piece	1000	1620	338	4089
25	Gearset	104	Ball	52100	--	0.7874-1.6535-0.4724	2-Piece	1000	1620	338	4581
26	Gearset	104	Ball	52100	--	0.7874-1.6535-0.4724	2-Piece	1000	1620	3368	4581
27	Gearset	104	Ball	52100	--	0.7874-1.6535-0.4724	2-Piece	1000	1620	338	4089
28	Gearset	104	Ball	52100	--	0.7874-1.6535-0.4724	2-Piece	1000	1620	338	4089
29	Gearset	104	Ball	52100	--	0.7874-1.6535-0.4724	2-Piece	1000	1620	338	4581
30	Gearset	104	Ball	52100	--	0.7874-1.6535-0.4724	2-Piece	1000	1620	338	4581

NOTES: (1) Life calculation based on vendor empirical formula.

6.2.1 Materials

Type 52100 high-chrome bearing steel is used for the needle roller and the radial ball bearing rings and balls.

6.2.2 Bearing Design

Bearing design and life calculations are based on the standards established by the Antifriction Bearing Manufacturers Association for ball and roller bearings except for the bearing size and stress calculations. Except where noted, these calculations are based on the high-speed ball and roller bearing program developed by A. B. Jones, Jr., and modified by Garrett to incorporate the method for life calculations described in AGMA Paper 229.19, "A Stress-Life Reliability Rating System for Gear and Rolling Element Bearing Compressive Stress, and Gear Root Bending Stress."

The Stress-Life-Reliability system includes the following parameters:

Material Quality - Dependent on the type of processing such as air melt, vacuum remelt, and multiple vacuum melt.

Material Hardness - The maximum hardness and the hardness tolerance range are used to determine the reference stress and the statistical distribution attributable to hardness variations.

Size - The size effect of a part is related to the distribution of weaknesses, flaws, or defects in the part. The larger the bearing, the greater the possibility of potentially weak areas or defects.

Accuracy - Accuracy variability is divided into two parts. The first covers the range of tolerances which are covered in the AFBMA class number. This includes concentricity, runout, bore, and outside diameter. The second covers the items not included in AFBMA Standard Control, such as the curvature tolerance in ball bearings and the crown configuration in roller bearings.

The four parameters listed above are used to generate a combined Wiebull exponent for the reliability variation with the maximum compressive stress.

The lubricant film thickness is used as a multiplying factor on the stress for a given number of stress cycles as a function of the specific film thickness (which is the ratio of EHD film thickness to surface roughness).

These parameters combine to generate the value of stress for a particular reliability at a life of 10^9 stressings. The system of AGMA 229.29 gives the shape of the curve of stress as a function of number of cycles, shaped to the experimental data for cycles approaching limits of one and infinity. This differs from the AFBMA method used in previous computer programs where the emprically-derived C, or specifice dynamic capacity if used as a reference point for a million revolutions, and an exponential relationship extrapolated to both high and low stresses. The AFBMA method yields unrealistic values outside a limited range.

Reliability

SECTION 7

RELIABILITY

7.1 RELIABILITY SUMMARY

Preliminary reliability and safety reviews of this actuation system show it to have a high reliability and safety potential. The key to good system reliability lies in a sound, well-conceived design. The GPSD SLEEC deployment drive design is such a design.

The proposed concept features components which are common in the aerospace industry for driving deployments and control surfaces. These components include ballscrew drives, flexible shaft drives, electric motors, brakes, and aircraft control cables. All the items have very high demonstrated reliability from vast experience levels. These components have proven reliability and have been successful over the years.

The analyses have been reviewed, and each part studied has a high margin of safety and all stresses are within aerospace industry accepted allowables. The system design has features which are very favorable to obtaining high reliability. The use of cable wraps avoids stress concentration points, minimizes shingle deflections, and converts the internal rocket exhaust pressure to usable torque for driving the deployment. The system is within a calculated torque of 200 in-lb_f of being balanced during the predicted 13-second deployment. The initial torques from the cable drums are in opposite rotations so that these torques cancel one another within the mounting blocks.

7.2 RELIABILITY PLAN

GPSD maintains a separate engineering organization in which reliability, maintainability and safety (RMS) are integrated. This RMS engineering group has been designated to be an advisory group to the individual engineering projects. The group is able to offer an unbiased evaluation of these closely-related diciplines. The expertise and direction exists for the performance of those specific tasks required to provide assurance from product design through service life. Input will continue throughout the design and development phases of the SLEEC program to quantify RMS predictions and considerations. The following are the minimum tasks required in the reliability program plan:

- Reliability predictions

- Failure mode, effects, and criticality analysis (FMECA)

- Failure reporting and corrective action (FRACA) system.

7.3 FUNCTIONAL COMPONENTS

The following paragraphs summarize the reliability comments by the functional components of the motor, brake, flexshaft drive, gearbox, ballscrew, cable drum, and aircraft cables.

7.3.1 Motor

The drive power requirements are very small as the design requires power only for ground checking and to assure initiation of deployment at launch. The generic failure rate for fractional horsepower motors in aerospace applications is 4.28×10^{-6} failures per hour.

7.3.2 Speed Control Brake and Stow Lock

Garrett has extensive brake experience, especially on thrust reversers of which over 7,800 have been produced. Field reliability is 30.2×10^{-6} failures per hour.

7.3.3 Flexible Drive Shafts

The use of flexible drive shafts to connect the individual driving motors, brakes, and gearboxes to form a hoop is a design of proven reliability. The basic design is used on the thrust reverser drives for the GE CF-6 engine for the McDonnell Douglas DC-10 and the Airbus A300. This application has a failure rate of 5.94×10^{-6} per hour based on field service. The reliability will be superior on the proposed SLEEC concept based on the short duration single-cycle mission. The continuous loop design makes the drive system redundant as one shaft could be completely severed and never compromise function.

7.3.4 Gearbox Drive

The gearbox drive system is specially designed to meet the requirements of the SLEEC actuation system. A review of the part analysis of the worm gear set, spur gear train, and internal planet gear reduction differential drive shows a conservatively designed system. The conservative design equates with high reliability. The run times and resulting cycles are several magnitudes lower than those generally found in Garrett's design history where service lives are typically in the thousands of hours. The lowest predicted gear life is one hour compared to a mission life of 13 seconds.

The bearings all have a calculated B1 life in excess of 95 hours in the gearbox drive system. All bearing parameters are well within the recommended operating envelope.

7.3.5 Ballscrew

Over 30,000 ballscrews have been designed and produced by The Garrett Corporation as components of engine thrust reverser drives. This represents around 95% of the combined commercial and military markets. The typical failure rate is 0.96×10^{-6} on the DC-10, A300 and the Boeing 747. The predicted reliability of the ballscrew would be even better on the SLEEC application. The anticipated curvature of the splined shaft resulting in internal rubbing will increase friction but will not affect deployment completion.

7.3.6 Cable Drum

The high stress level of the cable payoff drums is compensated for with the selection of a high-strength material such as AISI S7 tool-grade steel. The use of this material results in a minimum margin of safety of 0.162 for torque. The highest stressed bearing is the first (fore) bearing on the cable drums because the highest pressures are at the beginning of the cone extension. Each tier of cables must pass through the highest pressure zone, but the foremost tier remains in it.

The additive torque of each cable also makes the fore end of the drum subject to the maximum torque stress. The system is designed such that part of the torque could be taken at the other end.

7.3.7 Aircraft Cable

The use of aircraft cable with swaged-end hardware is a proven, reliable technology. The dominant location of failure is the attachment of the end hardware which will be minimized by following MIL-T-6117C. The ball end between the sleeve and drum has a maximum force of less than 100 pounds because the friction from the cable wraps still remains after full deployment.

The swaged threaded stud receives the full maximum cable tension of 1790 pounds. However, this load is well within the strength of the cable and fitting with a safety factor of 1.07. The inherent characteristics of the cable makes a very reliable component. The load is spread over many cables which can stretch to distribute the load to other cables in the unlikely occurence of a loose or fractured cable.

7.4 PREDICTED RELIABILITY

The SLEEC system is predicted to have a reliability or probability of success of 0.9999994. This is based on the conservative failure rates from the reliability analysis of the concept and at the run time of 30 seconds. Failure rates and reliability of each functional component are tabulated below. The system reliability is the product of the component reliabilities.

The conversions from failure rate to reliability are based on the following an equation for an exponential distribution:

$$R = e^{\lambda - \ t}$$

where

R = reliability

e = natural logarithm base

λ = failure rate

t = time

Component	Failure Rate	Predicted Reliability
	x 10^{-6} Hours	
Electric motor	4.28	0.99999996
Latch brake	30.26	0.99999975
Flex drive	5.94	0.99999995
Gearbox drive	4.50	0.99999996
Ballscrew	0.94	0.99999999
Cable drum	25.21	0.99999979
Aircraft cable	nil	
Total	71.13	0.99999941